Journal of Medicinal Chemistry

Article

pubs.acs.org/jmc

Ligand-Based Design, Synthesis, and Biological Evaluation of 2-Aminopyrimidines, a Novel Series of Receptor for Advanced Glycation End Products (RAGE) Inhibitors

Young Taek Han,[†] Gyeong-In Choi,[†] Dohyun Son,[‡] Nam-Jung Kim,[†] Hwayoung Yun,[†] Sujin Lee,[†] Dong Jo Chang,[†] Hyun-Seok Hong,[§] Hee Kim,[§] Hee-Jin Ha,[§] Young-Ho Kim,[§] Hyun-Ju Park,[‡] Jeewoo Lee,[†] and Young-Ger Suh*[,†]

[†]College of Pharmacy, Seoul National University, 599 Gwanak-ro, Gwanak-gu, Seoul 151-742, Korea

[‡]School of Pharmacy, Sungkyunkwan University, Suwon 440-746, Korea

[§]Medifron DBT, Sandanro 349, Danwon-Gu, Ansan-City, Gyeonggi-Do, 425-839, Korea

Supporting Information

ABSTRACT: Using the approach of ligand-based drug design, we discovered a novel series of 4,6-disubstituted 2-aminopyrimidines as RAGE inhibitors. In transgenic mouse models of AD, one of the 4,6-bis(4-chlorophenyl)pyrimidine analogs, **59**, significantly lowered the concentration of toxic soluble Aβ in the brain and improved cognitive function. SPR analysis confirmed the direct binding of **59** with RAGE, which should contribute to its biological activities via inhibition of the RAGE−Aβ interaction. We also predicted the binding mode of the 4,6-bis(4-chlorophenyl)pyrimidine analogs to the RAGE V-domain through flexible docking study.

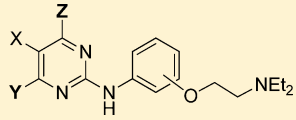

INTRODUCTION

Alzheimer's disease (AD) is one of the most common neurodegenerative diseases in elderly individuals. AD is characterized by progressive cognitive dysfunction and neuronal cell death, accompanied by an accumulation of extracellular amyloid-β (Aβ) plaques and intracellular neurofibrillary tangles in the brain.[1] Treatment with cholinesterase inhibitors, which results in the clinical improvement of memory and cognitive function, has been used as the first-line choice for AD to date. Recently a large number of preclinical and clinical studies focusing on various therapeutic targets involved in neuronal cell death, which is regarded as a fundamental cause of AD, have been performed. In particular, Aβ peptide is regarded as an important cytotoxic protein in the pathology of AD. Thus many current disease-modifying approaches for AD treatment focus on interrupting the pathological events related to the expression and accumulation of Aβ.[1b−e]

Aβ is produced primarily in somatic cells through the proteolysis of amyloid precursor protein (APP), and the entry of Aβ into the brain and its subsequent accumulation is essential for the pathogenesis of AD. Specific receptors and carrier-mediated transport systems at the BBB (blood−brain barrier) regulate the entry of the plasma-derived Aβ into the brain and the clearance of the brain-derived Aβ. Low-density lipoprotein receptor-related protein-1 (LRP-1) mediates the clearance of Aβ from the brain, and the receptor for advanced glycation end products (RAGE) is predominantly responsible for the plasma-derived Aβ influx into the brain.[2]

RAGE is a multiligand receptor on the cell surface that belongs to the immunoglobulin (Ig) superfamily. RAGE consists of an extracellular region, which is composed of one ligand-binding V-type Ig domain and two Ig-like C-domains, a short hydrophobic transmembrane-spanning region, and a signal-transducing cytoplasmic domain.[3] RAGE was originally identified as a receptor for the heterogeneous advanced glycation end products (AGE), which are generated under hyperglycemic conditions and lead to various diabetic complications. Along with the interactions of Aβ and AGE, the interactions of RAGE with the S100 protein family and the high-mobility group box-1 protein (HMGB1, also known as amphoterin) have been implicated in the pathogenesis of diverse chronic diseases such as rheumatoid arthritis, cardiovascular disease, and cancer. RAGE is expressed at low concentrations under normal physiological conditions except during embryonic development.[4] However, RAGE overexpression in diseased tissues is observed in most RAGE-related pathogenic conditions, which supports the possibility that RAGE can serve as a therapeutic target.[5]

In Alzheimer's disease, the RAGE−Aβ interaction not only promotes the transport of Aβ into the brain but also activates nuclear factor-κB (NF-κB), a transcription factor that plays a crucial role in various inflammatory responses. In addition, persistent RAGE hyperexpression arises from the positive feedback loop generated by the NF-κB-responsive element in the RAGE gene promoter.[6] The steady increase in Aβ accumulation and inflammation in the brain as the result of this vicious cycle aggravates AD. In this context, the inhibition of the RAGE−Aβ interaction, which decreases the rate of

Special Issue: Alzheimer's Disease

Received: February 8, 2012
Published: June 28, 2012

dx.doi.org/10.1021/jm300172z | J. Med. Chem. 2012, 55, 9120−9135

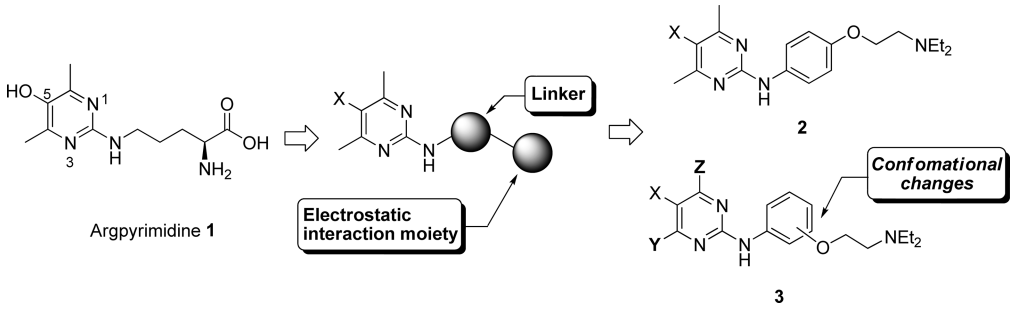

Figure 1. Structure of argpyrimidine **1** and overall strategy for the design of novel RAGE inhibitors.

deposition of Aβ and inhibits the inflammatory response to Aβ in the brain, has been recognized as a more preclusive and curative AD treatment strategy than the use of the current symptom-relief medications such as cholinesterase inhibitors.[1c] BBB permeability of a RAGE inhibitor might provide advantages such as an additional target inhibition,[7] although it is not essential to reach and inhibit the RAGE. Therefore, efforts toward the delivery of the RAGE inhibitors into the brain could be avoided, in contrast to other brain-targeting "disease-modifying agents" such as the metal chelators.[8] Despite such advantages for the inhibitors of the RAGE−Aβ interaction in AD treatment, there are not many reports on RAGE inhibitors to date. To the best of our knowledge, most studies of RAGE inhibition have focused on protein inhibitors such as sRAGE and RAGE antibodies.[5a] In the case of small-molecule RAGE inhibitors, one of Pfizer's compounds (PF-04494700) has reached a phase II clinical trial although the exact chemical structure has not yet been disclosed.[1d,9] Very recently, Zlokovic et al. reported a multimodal RAGE inhibitor during the preparation of our manuscript.[7]

Considering suggestions that there exist common or overlapping ligand binding sites in RAGE,[10] we assumed that all ligands for RAGE could serve as templates for the ligand-based design of RAGE inhibitors. However, most of the known ligands, except for monomeric AGE are macromolecules such as proteins and the secondary and tertiary structures of macromolecular ligands such as the β-sheet structure play a large role in the interaction with RAGE. It is also known that there is no essential difference in the binding with RAGE between the macromolecular and monomeric AGE.[11] Thus, monomeric AGEs, which generally consist of an *N*-heterocyclic moiety and an amino acid moiety as a part of the AGE−protein linkage,[12] were attractive as a template for the design of novel small-molecule RAGE inhibitors in terms of the structural simplicity and the chemical stability. In particular, argpyrimidine **1**, a monomeric AGE, was selected for design of the incipient RAGE inhibitors in the present study because the key structure of argpyrimidine seems to provide more synthetic accessibility and more drug-like features compared with that of other monomeric AGEs.[12b] Therefore, our ligand-based design of RAGE inhibitors commenced with an investigation of the two essential moieties of the argpyrimidine. The modification of the pyrimidine moiety and the appropriate replacement of the amino acid moiety, which was divided into the linker part and the terminal polar part, were extensively investigated. In addition, the effects of the overall conformational changes of the argpyrimidine analogs on the RAGE-inhibitory activities were also examined by changing the substitution pattern of the identified equivalents of the amino acid moiety (Figure 1). Finally, mechanistic studies for the identified RAGE inhibitors were performed and the binding modes of the RAGE inhibitors were also predicted by flexible docking studies. Herein, we report the ligand-based development of a novel series of 2-aminopyrimidines that are RAGE inhibitors that may serve as potential AD therapeutics.

CHEMISTRY

The synthesis route for the *N*-acyl and *N*-alkyl pyrimidol analogs is shown in Scheme 1. The ω-hydroxy-*N*-acyl analogs

Scheme 1. Synthesis of *N*-Acyl and *N*-Alkyl Pyrimidol Analogs[a]

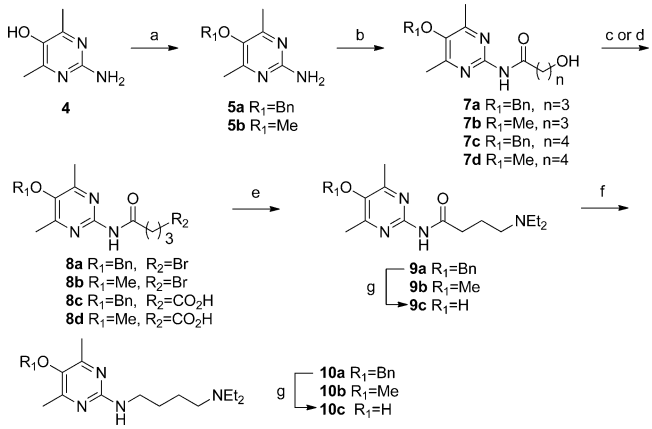

[a]Reagents and conditions: (a) BnBr or MeI, $CsCO_3$, CH_3CN, rt; (b) γ-butyrolactone or δ-valerolactone, Me_3Al, CH_2Cl_2, rt; (c) CBr_4, PPh_3, CH_2Cl_2/CH_3CN, rt; (d) CrO_3, aq. H_2SO_4/acetone, rt; (e) K_2CO_3, Et_2NH, rt; (f) LAH, THF, rt; (g) $Pd(OH)_2$, H_2, MeOH, rt.

7a−**7d** were prepared from the known pyrimidol **4**[13] by O-alkylation, followed by amidation via dimethylaluminum amide intermediates.[14] The treatment of alcohols **7a** and **7b** with carbon tetrabromide and amine substitution of the resulting bromides **8a** and **8b** furnished the *N*-acyl pyrimidol analogs **9a** and **9b**, respectively. Jones oxidation of alcohols **7c** and **7d** afforded the acids **8c** and **8d**, respectively. The *N*-acyl-5-hydroxy analog **9c** was produced by the debenzylation of **9a**. The reduction of amides **9a** and **9b** provided the *N*-alkyl pyrimidol analogs **10a** and **10b**, and the debenzylation of **10a** afforded the *N*-alkyl-5-hydroxy analog **10c**.

The *N*-aryl pyrimidol analogs **32** and **33** and the *N*-aryl pyrimidine analogs **34**−**60** were prepared via versatile coupling procedures from a variety of pyrimidine intermediates. The synthetic procedures for **32**−**60**, including the key aryl−aryl and aryl−amine couplings, are outlined in Schemes 2−6. For the synthesis of the *N*-aryl pyrimidine analogs, the 2-

dx.doi.org/10.1021/jm300172z | J. Med. Chem. 2012, 55, 9120−9135

Scheme 2. Synthesis of 2-Chloropyrimidine Intermediates[a]

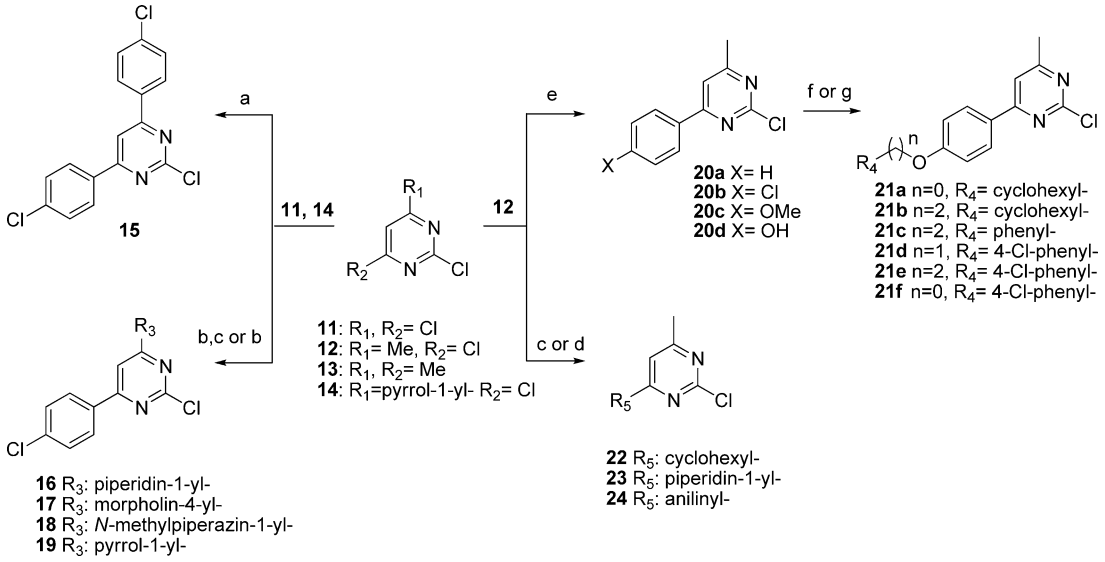

[a]Reagents and conditions: (a) 4-chlorophenylboronic acid (2.5 equiv), $Pd(PPh_3)_4$, Na_2CO_3, THF/H_2O, reflux; (b) 4-chlorophenylboronic acid (1.1 equiv), $Pd(PPh_3)_4$, Na_2CO_3, glyme/H_2O, 70 °C; (c) cyclic amines or aniline, EtOH, rt; (d) cyclohexylzinc bromide, $Pd(PPh_3)_4$, THF, reflux; (e) boronic acids, $Pd(PPh_3)_4$, Na_2CO_3, THF/H_2O, reflux; (f) $R_4(CH_2)_nOH$, diisopropyl azodicarboxylate, PPh_3, THF, rt; (g) 4-chlorophenylboronic acid, $Cu(OAc)_2$, Et_3N, 4 Å MS, CH_2Cl_2, rt.

chloropyrimidine intermediates **15**–**24** were initially prepared from the commercially available chloropyrimidines **11**–**13** or from pyrrolyl chloropyrimidine **14** by the appropriate combinations of the regioselective Suzuki reaction,[15] alkylation, and amination, as described in Scheme 2. The chloropyrimidine intermediate **15** was prepared from 2,4,6-trichloropyrimidine (**11**) by the Suzuki reaction using 2.5 equiv of boronic acid, whereas the N-substituted 2-chloropyrimidines **16**–**18** were synthesized by the Suzuki reaction in the presence of 1.1 equiv of boronic acid followed by amination with the corresponding amines. The 2-chloro-6-methyl pyrimidine intermediates **20** and **22**–**24** were prepared from 2,4-dichloro-6-methyl pyrimidine (**12**) by Pd(0)-catalyzed cross-coupling reactions (**20a**–**20d** and **22**) or amination (**23** and **24**). The 2-chloro-6-methyl pyrimidine intermediates **21a**–**21f** were prepared using the Mitsunobu[16] (**21a**–**21e**) or Ullmann reaction[17] (**21f**) with **20d**.

As shown in Scheme 3, the naphthyloxy intermediate **28** was prepared from 4-fluoroacetophenone **25** because the corresponding boronic acid was not commercially available. The sequential aromatic substitution of **25** and the Claisen condensation of **26** gave diketone **27**, which was subjected to condensation with urea and then chlorination of the resulting pyrimidol to afford chloropyrimidine **28**.[18]

For the synthesis of the *N*-aryl pyrimidol **33** and the *N*-aryl pyrimidine analogs **34**–**60**, the bromophenyl ether **30d** and the aminophenyl ethers **31a**–**31c** were prepared as described in Scheme 4. The Mitsunobu reaction of the commercially available nitrophenols **29a**–**29c** with *N*,*N*-diethyl ethanolamine and then the reduction of the nitro group afforded anilines **31a**–**31c**. Bromophenol **30d** was also prepared by the Mitsunobu reaction of commercially available 4-bromophenol (**29d**).

Finally, the coupling reactions of the pyrimidine intermediates with the corresponding aryl counterparts readily furnished the various *N*-aryl pyrimidine analogs. The Buckwald–Hartwig reaction of aminopyrimidine **5a** with **30d** afforded the *N*-aryl benzyloxypyrimidine **32**, which was converted into the pyrimidol analog **33** by debenzylation, as shown in Scheme 5. The *N*-aryl pyrimidine analogs **34**–**60** were prepared by the coupling reaction of the 2-chloropyrimidine intermediates with **31a**–**31c** under microwave irradiation conditions[19] as shown in Scheme 6.

Scheme 3. Synthesis of Naphthyloxyphenyl 2-Chloropyrimidine 28[a]

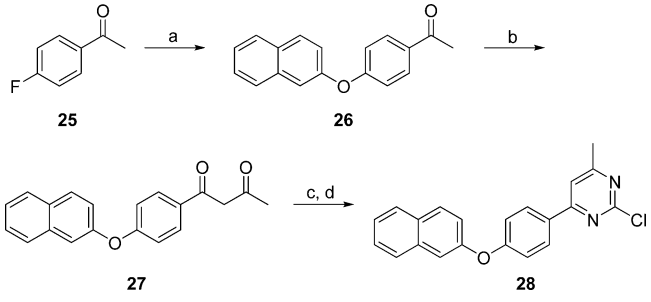

[a]Reagents and conditions: (a) naphthalen-2-ol, K_2CO_3, DMF, 120 °C; (b) EtOAc, EtOH, NaH, 18-crown-6, THF, reflux; (c) urea, *c*-HCl, EtOH, reflux; (d) $POCl_3$, reflux.

Scheme 4. Synthesis of Amino- and Bromophenyl Ethers[a]

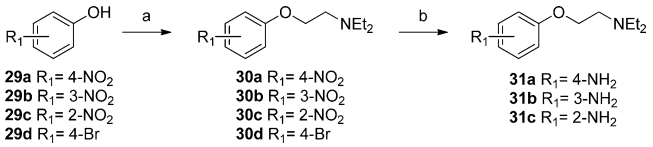

[a]Reagents and conditions: (a) *N*,*N*-diethyl ethanolamine, diisopropyl azodicarboxylate, PPh_3, THF, rt; (b) $SnCl_2 \cdot 2H_2O$, EtOH, reflux.

dx.doi.org/10.1021/jm300172z | *J. Med. Chem.* 2012, 55, 9120–9135

Scheme 5. Synthesis of *N*-Aryl Pyrimidol Analogs[a]

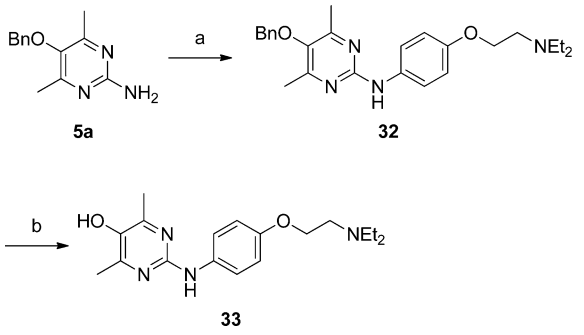

[a]Reagents and conditions: (a) $Pd(OAc)_2$, $CsCO_3$, 4,5-bis-(diphenylphosphino)-9,9-dimethylxanthene, **30d**, toluene, reflux; (b) $Pd(OH)_2$, H_2, MeOH, rt.

Scheme 6. Synthesis of *N*-Aryl Pyrimidine Analogs[a]

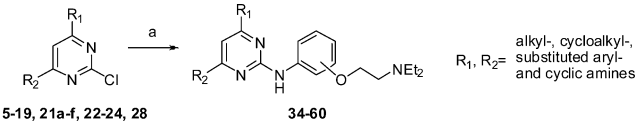

[a]Reagents and conditions: (a) **31a–31c**, 4 N HCl in dioxane, *n*-BuOH, 160 °C (microwave irradiation).

RESULTS AND DISCUSSION

Discovery of Novel Scaffolds for RAGE Inhibitors. Our initial strategy for the development of new RAGE inhibitors focused on the appropriate alteration of the 2-aminopentanoic acid moiety of argpyrimidine **1**. Thus, our modification of 2-aminopentanoic acid commenced with the identification of the appropriate equivalents of the propyl linker part and the terminal amino acid as the polar part. The synthesized analogs were evaluated for their RAGE–Aβ interaction inhibitory activity using an enzyme-linked immunosorbent assay (ELISA). In brief, Aβ was incubated with biotinylated RAGE on a streptavidin-coated plate in the presence of each analog. After the unbound Aβ was washed off the plate, to evaluate the RAGE inhibitory activity of the analog, the amount of remaining Aβ was measured using horseradish peroxidase-conjugated Aβ specific antibody (see the Experimental Section and Supporting Information Figure S1). Unfortunately, as shown in Table 1, the analogs of carboxylic acids, alcohols, and amines with alkyl and acyl linkers did not exhibit the desired activity for RAGE inhibition, even though we predicted that these compounds would form hydrogen bonds or electrostatic interactions with the basic residues of RAGE ligand binding site.[11] Only amine analogs **32–34**, which have an alkoxyaryl linker, exhibited weak inhibitory activities regardless of the phenol protection. Thus, we turned our attention to intensive optimization of the pyrimidine scaffold with the alkoxyaryl-amine side chain.

Structure–Activity Relationship of the *N*-Aryl Pyrimidine Analogs. Because we observed no substituent effects of the hydroxyl group of the pyrimidol analogs **32–34**, we focused on the substituent effects at the 4- and 6-positions of the pyrimidine core on the RAGE inhibitory activities. In addition, we investigated the conformational effects on the inhibitory activities by changing the substitution positions of the side chain of the alkoxyaryl linker as shown in Table 2.

Table 1. In Vitro Activities of the Initial 4,6-Dimethyl Pyrimidin-5-ol Analogs

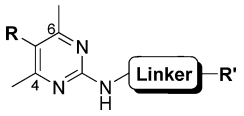

Analogs	R	Linker	R'	% Inhibition[a]
8c	-OBn	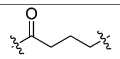	-CO_2H	NA[b]
8d	-OMe	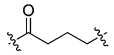	-CO_2H	NA
7a	-OBn	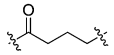	-OH	NA
7b	-OMe	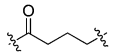	-OH	NA
9a	-OBn	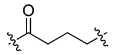	-NEt_2	NA
9b	-OMe	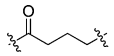	-NEt_2	NA
9c	-OH	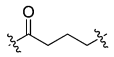	-NEt_2	NA
10a	-OBn	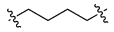	-NEt_2	NA
10b	-OMe	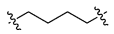	-NEt_2	NA
10c	-OH	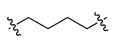	-NEt_2	NA
32	-OBn	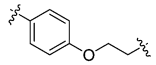	-NEt_2	14.6 ± 1.2
33	-OH	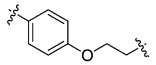	-NEt_2	16.2 ± 4.1
34	-H	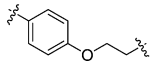	-NEt_2	16.0 ± 0.5

[a]Percent inhibition values were determined by duplicate experiments using 20 μM of the synthesized analogs and are expressed as the means ± standard deviation. [b]NA indicates not active.

First, we investigated monosubstitution at the 4-position (**36–44**) of the pyrimidine core. Generally, the introduction of cyclic substituents at the 4-position increased the inhibitory activities regardless of the electronic character of the substituents. Interestingly, analog **43**, which possesses an aminoethoxy substituent at the *meta*-position of the aniline side chain, exhibited better inhibitory activity than the *para*-substituted analog **42**, whereas the *ortho*-substituted analog **44** exhibited a higher inhibitory activity than the *meta*- and *para*-substituted analogs. These results partly confirmed that there is a conformational effect of the side chain on the RAGE inhibitory activities. The conformational effects on the inhibition were also observed in the *para*-substituted analog **34** and the *meta*-substituted analog **35** in the 4,6-dimethylpyrimidine series. We extended our studies on the substituent effects to substituent elongation at the 4-position of the pyrimidine core (**45–53**). Elongation with an additional aryloxy (**45**) or arylalkoxy moiety (**46–49**) significantly

dx.doi.org/10.1021/jm300172z | J. Med. Chem. 2012, 55, 9120–9135

Table 2. In Vitro Activities of the Synthesized Analogs

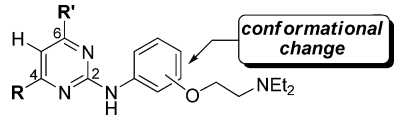

Analogs	R	R'	Substitution position	% Inhibition[a] (IC_{50})
35	-Me	-Me	*meta*	20.8 ± 4.6
36		-Me	*para*	30.6 ± 3.6
37		-Me	*para*	43.3 ± 1.5
38		-Me	*para*	32.7 ± 2.1
39		-Me	*para*	33.0 ± 7.6
40	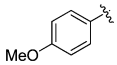	-Me	*para*	31.7 ± 2.6
41	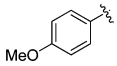	-Me	*meta*	30.9 ± 7.2
42	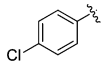	-Me	*para*	37.1 ± 5.8
43	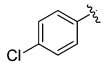	-Me	*meta*	41.6 ± 0.8
44	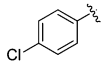	-Me	*ortho*	47.2 ± 2.7
45	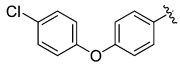	-Me	*para*	21.1 ± 0.6
46	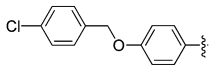	-Me	*para*	12.7 ± 3.5
47	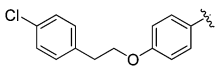	-Me	*para*	NA[b]
48	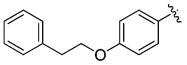	-Me	*para*	NA
49	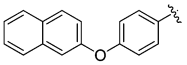	-Me	*para*	21.4 ± 5.1
50	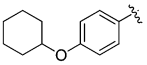	-Me	*para*	32.6 ± 1.7
51	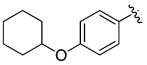	-Me	*meta*	45.6 ± 4.9
52	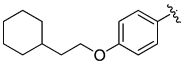	-Me	*para*	32.7 ± 4.4
53	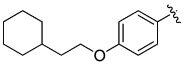	-Me	*meta*	49.6 ± 4.4
54	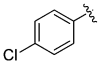		*meta*	17.1 ± 8.3
55	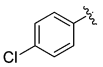		*meta*	3.1 ± 1.6
56	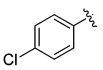		*meta*	4.5 ± 0.2
57	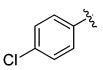		*meta*	26.3 ± 0.5
58	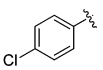	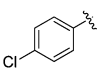	*para*	33.6 ± 1.4
59	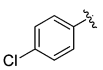	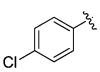	*meta*	54.0 ± 1.6 (16.5μM)
60	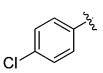	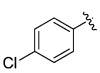	*ortho*	70.8 ± 3.8 (4.6μM)

[a]Percent inhibition values were determined by duplicate experiments using 20 μM of the synthesized analogs and are expressed as the means ± standard deviations. [b]NA indicates not active.

decreased or eliminated the inhibitory activity, whereas elongation with an alicyclic chain (**50**–**52**) provided equipotent activities or slightly improved activities (**53**) for both the *meta*- and *para*-substituents. The inhibitory activities decreased as the length of the aliphatic linker between the two aromatic moieties increased (**45**–**47**). The disappearance of the inhibitory activities of the phenethyl ether analogs **47** and **48** is likely due to folding resulting from an intramolecular π–π interaction involving the biaryl ether moiety. We further investigated the disubstitution effect at the 4- and 6-positions based on the monosubstituted analogs **42**–**44**, which exhibited potent inhibitory activities. Disappointingly, all of the cyclic amine-substituted analogs (**54**–**57**) exhibited weak or poor inhibitory activities. However, the disubstituted analogs possessing the 4-chlorophenyl substituent (**58**–**60**) exhibited dramatically increased activities regardless of the substitution position of the aminoethoxy chain. In particular, the disubstituted analogs with aminoethoxy chains at the *meta*- and *ortho*-positions exhibited excellent inhibitory activities, with IC_{50} values of 16.5 (**59**) and 4.6 μM (**60**), respectively. These results further supported the existence of conformational effects of the side chain on the RAGE inhibitory activities of the pyrimidine analogs.

In Vivo Studies. We performed further in vivo studies on the pyrimidine analogs **53**, **59**, and **60**, which showed high in vitro RAGE inhibitory activities. In an NF-κB reporter assay using the C6 glioma cells, we observed that the Aβ-induced NF-κB signaling was down-regulated by all three analogs

dx.doi.org/10.1021/jm300172z | J. Med. Chem. 2012, 55, 9120–9135

Table 3. Preliminary in Vivo Assay of the Inhibition of Aβ Brain Entry in an Acute Model[a]

	53[b]+Aβ, Aβ only	59[c]+Aβ, Aβ only	60[b]+Aβ, Aβ only
human Aβ in brain[d]	126.78 ± 24.60, 144.27 ± 16.07	66.52 ± 8.74,[f] 101.30 ± 11.15	74.03 ± 27.60, 90.62 ± 12.30
% reduction	12.1	34.3	18.3
human Aβ in plasma[e]	1766.03 ± 239.07, 1861.19 ± 276.99	1027.00 ± 103.90, 1066.00 ± 57.35	1504.32 ± 463.39, 1547.63 ± 477.68
% reduction	5.0	3.7	2.8

[a]The amount of human Aβ in the brain and the plasma of mice was measured following tail vein injection of vehicle or the analogs. The concentrations of human Aβ of mice are expressed as the means ± standard deviation. [b]25 mg/kg, n = 4, male. [c]25 mg/kg, n = 7, male. [d]pg/mg protein of the brain extracts. [e]ng/mL of plasma [f]$P < 0.05$.

Table 4. Inhibition of Aβ Accumulation[a] in the Brain of Mice and the Improvement in Cognitive Function by Analog 59 in an AD Model

	soluble $Aβ_{1-40}$	insoluble $Aβ_{1-40}$	soluble $Aβ_{1-42}$	insoluble $Aβ_{1-42}$	Y maze[b]
vehicle (n = 5)	8.66 ± 1.81	137.38 ± 58.13	17.34 ± 5.17	513.73 ± 219.56	50.95 ± 10.8
59 (n = 4)	6.25 ± 0.65[c]	98.49 ± 11.68	12.04 ± 1.87[c]	354.25 ± 65.18	63.60 ± 6.6[c]

[a]The concentrations are expressed as the means ± standard deviation (ng/mg protein of brain extract). [b]Spontaneous alternation percentage. [c]$P < 0.05$.

without cytotoxicity at the indicated concentrations (see the Supporting Information Figure S3). We also performed an acute model study on the three analogs to confirm the desired inhibition of Aβ brain entry. The acute model was designed based on a previous report that revealed a dominant role of RAGE in the transport of peripheral Aβ into brain.[20] In brief, each RAGE inhibitor was injected intraperitoneally prior to an injection of human Aβ into wild-type mice, and then the inhibitory activities were estimated by measuring the level of human Aβ in the brain extracts of the mice. As shown in Table 3, all three analogs exhibited brain Aβ-lowering effects without significant changes of the amount of peripheral human Aβ. These observations obviously supported that the Aβ brain entry was inhibited by the pyrimidine analogs via their RAGE inhibition. Further long-term studies using the AD model and analog **59**, which exhibited the most potent Aβ brain-entry inhibition in acute model, were performed to validate the desired therapeutic effects of the pyrimidine analogs. The results are shown in Table 4. The efficacy of **59** in the AD model study was evaluated based on Aβ accumulation in the brain and the subsequent improvement in cognitive function. As expected, after oral administration of **59** for 3 months, we observed that analog **59** effectively lowered the Aβ brain accumulation, including the accumulation of insoluble Aβ (also see the Supporting Information Figure S2) and soluble Aβ (particularly toxic soluble Aβ1−42),[21] and improved the cognitive function without significant side effects such as lethality.

Studies on the Binding of the RAGE-Inhibitory Analogs with RAGE. We investigated the mechanism of RAGE inhibition by analog **59** as a representative inhibitor. Using surface plasmon resonance (SPR),[11] the binding of **59** with RAGE fixed on a sensor chip was observed in a dose-dependent manner with a K_D value of 1.02×10^{-4} M, as shown in Figure 2. This observation supported the direct binding of **59** with RAGE, which would contribute to its RAGE inhibitory activity and the subsequent inhibition of Aβ accumulation in the brain.

Along with the SPR analysis, a docking study of the 4,6-diarylpyrimidine analogs **58**−**60** on RAGE was performed based on the results of the in vitro assays. The X-ray structure of RAGE was retrieved from the PDB (ID 3O3U),[22] and the active site was defined within a 3.0 Å radius of the specific

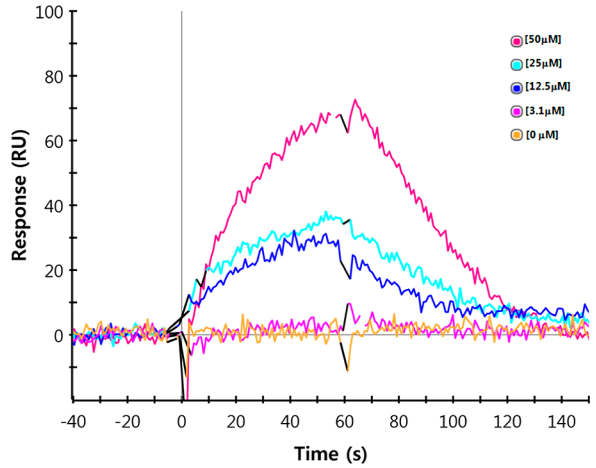

Figure 2. SPR study on the binding of analog **59** with RAGE. The real-time interaction of **59** with biotinylated RAGE was assessed by measuring the surface plasmon resonance (SPR). RU, resonance units. Typical SPR response curves were measured using a series of concentrations of the tested compounds. The response values were normalized by subtracting the response value of the empty channel. The kinetic and equilibrium constants, shown in the text, were obtained by a global fit, using the Langmuir 1:1 bimolecular kinetic model.

amino acid residues (Lys43, Lys44, Arg48, and Arg104), taking into account their important roles described in the literature.[11,23] As shown in Figure 3, the key residues showed important properties that allowed them to interact with **58**−**60**. Interestingly, the Surflex-Dock docking analysis revealed a good correlation with the in vitro data in terms of the binding energy scores as shown in Table 5. The *ortho*-isomer **60** (magenta), which exhibited the best in vitro activity, formed hydrogen bonds between the nitrogen of the pyrimidine core and Arg104 of the receptor (yellow dotted line). With respect to the binding energy scores, analog **60** also had the highest score (−log K_d = 7.73). The binding energy score of the *meta*-isomer **59** (orange) was ranked second (−log K_d = 6.23), although this compound formed various hydrogen bonds not only with Arg104 but also with Arg48 and Met102 (dotted red lines). These results are likely due to the orientation of the electronegative 4-chlorophenyl moiety of **60**, which was close to Lys43 and Lys44, which form a positively charged area in the

dx.doi.org/10.1021/jm300172z | J. Med. Chem. 2012, 55, 9120−9135

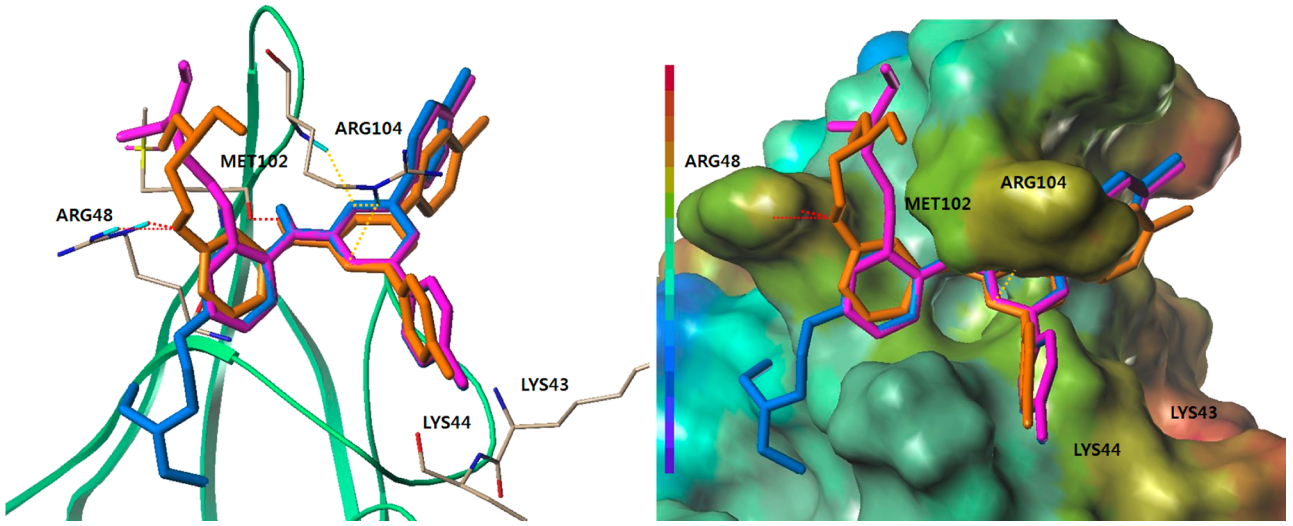

Figure 3. Predicted binding modes of the 4,6-diphenylpyrimidine analogs **58**–**60** on the RAGE V-domain. Superpositioning of the docking poses of **58**–**60** in the binding site of RAGE obtained by Surflex-Dock. (left) Ligand atoms are rendered in capped stick. The colors are as follows: **58** in blue, **59** in orange, and **60** in magenta. Yellow dotted lines indicate common hydrogen bonds between each compound and the receptor. Red dotted lines are additional hydrogen bonds of **59** with the receptor. Key residues of the receptor are shown in stick (gray carbon). Green cartoons represent the backbone of RAGE. (right) The surface of RAGE was rendered based on the electrostatic properties; a color gradient from red to violet is used to color the molecular surface, where red and violet are for positive and negative electrostatic surface potential, respectively.

Table 5. Binding Energy Scores of 58–60 and Comparisons with Their in Vitro Activities

	58	59	60
binding score[a]	6.09	6.23	7.73
in vitro activity[b]	33.6	54.0	70.8

[a]Binding scores are expressed in $-\log K_d$ values. [b]Percent inhibition by 20 μM analogs.

ligand binding site. The *para*-isomer **58** (blue) was ranked third in terms of the in vitro activity and the binding energy score ($-\log K_d$ = 6.09). We assumed that the inappropriate orientation of the diethylaminoethyl ether moiety of **58**, in comparison with that of *ortho* and *meta* isomers, might induce weaker binding and thus lower activity.

CONCLUSION

In connection with the development of novel RAGE inhibitors as potential AD therapeutics, we designed and synthesized a series of 2-aminopyrimidines on the structural basis of argpyrimidine, a monomeric AGE. Subsequently, we identified the 4,6-disubstituted 2-aminopyrimidine core as a novel scaffold for RAGE-inhibitory activity. We also established the structure–activity relationship of the inhibitors based on the in vitro RAGE inhibition. In particular, we identified the pyrimidine analogs **53**, **59**, and **60** as promising RAGE inhibitors. These compounds exhibited excellent in vitro activities and good in vivo activities in the acute model. Moreover, analog **59** resulted in significant inhibition of Aβ (especially toxic soluble Aβ) accumulation in the brain and in a noticeable improvement in cognitive function in a mouse AD model with oral administration. The mechanism of the RAGE inhibitory activities of the 2-aminopyrimidine analogs was partly elucidated by SPR analysis, the results of which support the hypothesis that the direct binding of the representative inhibitor **59** with RAGE contribute to its RAGE-inhibitory activities. In addition, the binding mode of the inhibitors with RAGE was predicted by a docking study of the 4,6-diarylpyrimidine analogs **58**–**60** on the RAGE V-domain.

EXPERIMENTAL SECTION

Chemistry. Unless noted otherwise, all starting materials and reagents were obtained commercially and were used without further purification. Tetrahydrofuran was distilled from sodium benzophenone ketyl. Dichloromethane and acetonitrile were freshly distilled from calcium hydride. All solvents used for routine product isolation and chromatography were of reagent grade and glass distilled. Reaction flasks were dried at 100 °C before use, and air- and moisture-sensitive reactions were performed under argon. Flash column chromatography was performed using silica gel 60 (230–400 mesh, Merck) with the indicated solvents. Thin-layer chromatography was performed using 0.25 mm silica gel plates (Merck). Mass spectra were obtained using a VG Trio-2 GC-MS instrument, and high resolution mass spectra were obtained using a JEOL JMS-AX 505WA unit. ^{1}H and ^{13}C spectra were recorded on a JEOL JNM-LA 300, Bruker Analytik ADVANCE digital 400, ADVANCE digital 500, or JEOL ECA-600 spectrometer in deuteriochloroform ($CDCl_3$), deuteriomethanol (CD_3OD), or deuterated dimethyl sulfoxide (DMSO-d_6). Chemical shifts are expressed in parts per million (ppm, δ) downfield from tetramethylsilane and are referenced to the deuterated solvent ($CHCl_3$). ^{1}H NMR data are reported in the order chemical shift, multiplicity (s, singlet; bs, broad singlet; d, doublet; t, triplet; q, quartet; m, multiplet or multiple resonance), numbers of protons, and coupling constants in hertz (Hz). All the final compounds were purified up to more than 95% purity. The purities were determined by a reverse-phase high-performance liquid chromatography using Eclipse Plus C18 (4.6 × 250 mm^2) with an isocratic flow at 1 mL/min. The detail analytical conditions are available in Supporting Information.

*5-(Benzyloxy)-4,6-dimethylpyrimidin-2-amine (**5a**).* To a solution of **4** (100 mg, 0.72 mmol) and $CsCO_3$ (352 mg, 1.08 mmol) in acetonitrile (10 mL) was added benzyl bromide (0.12 mL, 0.94 mmol). The reaction mixture was stirred for 5 h at ambient temperature and filtered using a Celite pad. The mixture was concentrated *in vacuo* and then diluted with EtOAc. The organic layer was washed with water and brine, and the aqueous phase was extracted with EtOAc several times. The combined organic layer was dried over $MgSO_4$ and concentrated *in vacuo*. Purification of the residue via flash column chromatography on silica gel (EtOAc/*n*-

dx.doi.org/10.1021/jm300172z | J. Med. Chem. 2012, 55, 9120–9135

hexane = 2:1) afforded 135 mg (82%) of **5a** as a white solid with a melting point of 134−136 °C. ^{1}H NMR (300 MHz, $CDCl_3$) δ 7.38−7.36 (m, 5H), 4.74 (bs, 4H), 2.28 (s, 6H). LRMS (FAB) m/z 230 (M + H$^+$).

*5-Methoxy-4,6-dimethylpyrimidin-2-amine (**5b**).* Amine **5b** was prepared from **4** (1.0 g, 7.19 mmol) by the procedure for **5a**, using iodomethane (0.58 mL, 9.34 mmol) instead of benzyl bromide. Purification of the residue via flash column chromatography on silica gel (EtOAc/*n*-hexane = 2:1) afforded 859 mg (78%) of **5b** as a yellow solid with a melting point of 94−98 °C. ^{1}H NMR (300 MHz, $CDCl_3$) δ 4.72 (bs, 2H), 3.64 (s, 3H), 2.31 (s, 6H). LRMS (FAB) m/z 154 (M + H$^+$).

*N-(5-(Benzyloxy)-4,6-dimethylpyrimidin-2-yl)-4-hydroxybutanamide (**7a**).* To a solution of **5a** (20 mg, 0.09 mmol) in CH_2Cl_2 (2 mL) at ambient temperature was added trimethylaluminum (0.05 mL of 2 M solution in toluene, 0.10 mmol) dropwise. The resulting yellowish mixture was stirred for 20 min, and then γ-butyrolactone (23 mg, 0.26 mmol) in CH_2Cl_2 (1 mL) was added slowly. The reaction mixture was stirred overnight, diluted with EtOAc, and quenched with 10% aqueous citric acid and Rochelle's solution. The aqueous phase was extracted with EtOAc several times. The combined organic layer was washed with water and brine, dried over $MgSO_4$, and concentrated *in vacuo*. Purification of the residue via flash column chromatography on silica gel (EtOAc/*n*-hexane = 3:1) afforded 17 mg (62%) of **7a** as a colorless oil. ^{1}H NMR (300 MHz, $CDCl_3$) δ 8.06 (s, 1H), 7.39 (bs, 5H), 4.80 (s, 2H), 3.73 (t, 2H, J = 5.8 Hz), 2.87−2.85 (m, 2H), 2.38 (s, 6H), 2.03−1.97 (m, 2H). ^{13}C NMR ($CDCl_3$, 75 MHz) δ 176.4, 161.8, 161.8, 151.9, 146.4, 136.1, 128.8, 128.8, 128.7, 128.2, 128.2, 75.5, 62.1, 33.5, 27.8, 19.1, 19.1. LRMS (FAB) m/z 316 (M + H$^+$). HRMS (FAB) calcd for $C_{17}H_{22}N_3O_3$ (M + H$^+$): 316.1656; found 316.1652.

*4-Hydroxy-N-(5-methoxy-4,6-dimethylpyrimidin-2-yl)-butanamide (**7b**).* Amide **7b** was prepared by the procedure for **7a**, using **5b** (1.0 g, 6.52 mmol) instead of **5a**. Purification of the residue via flash column chromatography on silica gel (EtOAc only) afforded 1.1 g (71%) of **7b** as a colorless oil. ^{1}H NMR (500 MHz, $CDCl_3$) δ 8.23 (bs, 1H), 3.72−3.70 (m, 5H), 2.85 (bs, 2H), 2.78 (bs, 1H), 2.41 (s, 6H), 2.00−1.95 (m, 2H). LRMS (FAB) m/z 240 (M + H$^+$). ^{13}C NMR ($CDCl_3$, 75 MHz) δ 173.6, 161.4, 161.4, 151.7, 147.7, 62.0, 60.6, 33.5, 27.8, 18.7, 18.5. HRMS (FAB) calcd for $C_{11}H_{18}N_3O_3$ (M + H$^+$): 240.1343; found 240.1336.

*N-(5-(Benzyloxy)-4,6-dimethylpyrimidin-2-yl)-5-hydroxypentanamide (**7c**).* Amide **7c** was prepared from **5a** (1.0 g, 4.36 mmol) by the procedure for **7a**, using δ-valerolactone (0.6 mL, 6.54 mmol) instead of γ-butyrolactone. Purification of the residue via flash column chromatography on silica gel (EtOAc/*n*-hexane = 3:1) afforded 1.0 g (71%) of **7c** as a colorless oil. ^{1}H NMR (300 MHz, $CDCl_3$) δ 8.76 (s, 1H), 7.40−7.30 (m, 5H), 4.77 (s, 2H), 3.64−3.61 (m, 2H), 2.72−2.70 (m, 2H), 2.36 (s, 6H), 1.82−1.72 (m, 2H), 1.67−1.58 (m, 2H). LRMS (FAB) m/z 330 (M + H$^+$). HRMS (FAB) calcd for $C_{18}H_{24}N_3O_3$ (M + H$^+$): 330.1812; found 330.1821.

*5-Hydroxy-N-(5-methoxy-4,6-dimethylpyrimidin-2-yl)-pentanamide (**7d**).* Amide **7b** was prepared from **5b** (500 mg, 3.26 mmol) by the procedure for **7b**, using δ-valerolactone (0.45 mL, 4.89 mmol) instead of γ-butyrolactone. Purification of the residue via flash column chromatography on silica gel (EtOAc only) afforded 585 mg (71%) of **7d** as a colorless oil. ^{1}H NMR (300 MHz, $CDCl_3$) δ 8.24 (bs, 1H), 3.74−3.66 (m, 5H), 2.85−2.81 (m, 2H), 1.84−1.54 (m, 4H). LRMS (FAB) m/z 254 (M + H$^+$).

*N-(5-(Benzyloxy)-4,6-dimethylpyrimidin-2-yl)-4-bromobutanamide (**8a**).* To a solution of **7a** (24 mg, 0.08 mmol) and triphenylphosphine (28 mg, 0.11 mmol) in CH_2Cl_2/CN_3CN (1:1, 2 mL) at ambient temperature was added carbon tetrabromide (38 mg, 0.12 mmol). The reaction mixture was stirred for 5 h and diluted with CH_2Cl_2 (10 mL). The organic layer was washed with water and brine, dried over $MgSO_4$, and concentrated *in vacuo*. Purification of the residue via flash column chromatography on silica gel (EtOAc/*n*-hexane = 1:3) afforded 27 mg (96%) of **8a** as a white solid with a melting point of 149−152 °C. ^{1}H NMR (300 MHz, $CDCl_3$) δ 8.60 (bs, 1H), 7.42−7.34 (m, 5H), 4.83 (s, 2H), 3.53 (t, 2H, J = 6.4 Hz), 2.92−2.90 (m, 2H), 2.41 (s, 6H), 2.31−2.22 (m, 2H). LRMS (FAB) m/z 378 (M + H$^+$).

*4-Bromo-N-(5-methoxy-4,6-dimethylpyrimidin-2-yl)butanamide (**8b**).* Amide **8b** was prepared by the procedure for **8a**, using **7b** (78 mg, 0.33 mmol) instead of **7a**. Purification of the residue via flash column chromatography on silica gel (EtOAc/*n*-hexane = 1:1) afforded 97 mg (97%) of **8b** as a yellow oil. ^{1}H NMR (300 MHz, $CDCl_3$) δ 7.92 (bs, 1H), 3.71 (s, 3H), 3.53 (t, 2H, J = 6.2 Hz), 2.98−2.90 (m, 2H), 2.42 (s, 6H), 2.30−2.21 (m, 2H). LRMS (FAB) m/z 302 (M + H$^+$).

*5-((5-(Benzyloxy)-4,6-dimethylpyrimidin-2-yl)amino)-5-oxopentanoic acid (**8c**).* Initially, *c*-H_2SO_4 (20 mL) was slowly added to a solution of CrO_3 (3 g) in water (30 mL), and 0.4 M chromic acid was prepared by addition of water to the above mixture up to total volume of 75 mL. To a solution of **7c** (18 mg, 0.06 mmol) in acetone (5 mL) was added the 0.4 M chromic acid (0.1 mL) at ambient temperature. The reaction mixture was stirred for 30 min at ambient temperature, concentrated *in vacuo*, and then diluted with EtOAc. The organic layer was washed with water and brine, dried over $MgSO_4$, and concentrated *in vacuo*. Purification of the residue via flash column chromatography on silica gel (MeOH/CH_2Cl_2 = 1:9) afforded 7 mg (37%) of **8c** as a white solid with a melting point of 168−173 °C. ^{1}H NMR (300 MHz, CD_3OD) δ 7.44−7.35 (m, 5H), 4.88 (s, 2H), 2.54 (t, 2H, J = 7.3 Hz), 2.42−2.36 (m, 8H), 1.97 (t, 2H, J = 7.3 Hz). LRMS (FAB) m/z 344 (M + H$^+$). ^{13}C NMR ($CDCl_3$, 75 MHz) δ 180.1, 170.3, 161.9, 161.9, 152.1, 146.1, 136.2, 128.8, 128.8, 128.8, 128.2, 128.2, 64.0, 28.7, 27.4, 23.8, 18.6, 18.6. HRMS (FAB) calcd for $C_{18}H_{22}N_3O_4$ (M + H$^+$): 344.1605; found 344.1610.

*5-((5-Methoxy-4,6-dimethylpyrimidin-2-yl)amino)-5-oxopentanoic acid (**8d**).* Acid **8d** was prepared by the procedure for **8c**, using **7d** (50 mg, 0.20 mmol) instead of **7c**. Purification of the residue via flash column chromatography on silica gel (MeOH/CH_2Cl_2 = 1:6) afforded 23 mg (43%) of **8d** as a white solid with a melting point of 132−137 °C. ^{1}H NMR (300 MHz, $CDCl_3$) δ 3.70 (s, 3H), 2.70 (t, 2H, J = 7.5 Hz), 2.53−2.43 (m, 8H), 2.06−1.98 (m, 2H). ^{13}C NMR ($CDCl_3$, 100 MHz) δ 178.1, 171.3, 161.6, 161.6, 152.0, 152.0, 60.7, 35.8, 32.3, 19.7, 18.2, 18.2. LRMS (FAB) m/z 268 (M + H$^+$). HRMS (FAB) calcd for $C_{12}H_{18}N_3O_4$ (M + H$^+$): 268.1292; found 268.1312.

*N-(5-(Benzyloxy)-4,6-dimethylpyrimidin-2-yl)-4-(diethylamino)-butanamide (**9a**).* A solution of **8a** (15 mg, 0.04 mmol) and K_2CO_3 (28 mg, 0.2 mmol) in diethylamine (0.5 mL) was stirred for 12 h at ambient temperature and diluted with EtOAc (10 mL). The organic layer was washed with saturated NH_4Cl solution and brine, dried over $MgSO_4$, and concentrated *in vacuo*. Purification of the residue via flash column chromatography on silica gel (MeOH/CH_2Cl_2 = 1:6) afforded 6 mg (40%) of **9a** as a yellow oil. ^{1}H NMR (300 MHz, $CDCl_3$) δ 7.40−7.33 (m, 5H), 4.78 (s, 2H), 2.65−2.54 (m, 8H), 1.91−1.81 (m, 2H), 1.05 (t, 6H, J = 7.1 Hz). ^{13}C NMR ($CDCl_3$, 75 MHz) δ 172.4, 161.4, 161.4, 152.3, 146.2, 136.2, 128.7, 128.7, 128.6, 128.1, 128.1, 75.4, 52.2, 46.4, 46.4, 36.1, 21.9, 19.2, 19.2, 10.8, 10.8. LRMS (FAB) m/z 371 (M + H$^+$). HRMS (FAB) calcd for $C_{21}H_{31}N_4O_2$ (M + H$^+$): 371.2442; found 371.2435.

*4-(Diethylamino)-N-(5-methoxy-4,6-dimethylpyrimidin-2-yl)-butanamide (**9b**).* Amide **9b** was prepared by the procedure for **9a**, using **8b** (35 mg, 0.12 mmol) instead of **8a**. Purification of the residue via flash column chromatography on silica gel (MeOH/CH_2Cl_2 = 1:4) afforded 13 mg (39%) of **9b** as a yellow oil. ^{1}H NMR (300 MHz, $CDCl_3$) δ 3.69 (s, 3H), 2.61−2.50 (m, 8H), 2.41 (s, 6H), 1.85−1.81 (m, 2H), 1.03 (t, 6H, J = 7.1 Hz). ^{13}C NMR ($CDCl_3$, 75 MHz) δ 172.6, 160.9, 160.9, 152.2, 147.4, 60.4, 52.2, 46.3, 46.3, 36.1, 22.1, 18.7, 18.7, 11.0, 11.0. LRMS (FAB) m/z 295 (M + H$^+$). HRMS (FAB) calcd for $C_{15}H_{27}N_4O_2$ (M + H$^+$): 295.2129; found 295.2135.

*4-(Diethylamino)-N-(5-hydroxy-4,6-dimethylpyrimidin-2-yl)-butanamide (**9c**).* A suspension of **9a** (12 mg, 0.03 mmol) and 20% $Pd(OH)_2$ (3 mg) in MeOH (5 mL) was stirred for 3 h under H_2 at ambient temperature. The reaction mixture was filtered through a Celite pad and concentrated *in vacuo*. Purification of the residue via flash column chromatography on silica gel (MeOH/CH_2Cl_2 = 1:1) afforded 7.1 mg (79%) of **9c** as a colorless oil. ^{1}H NMR (300 MHz, CD_3OD) δ 3.02−2.90 (m, 6H), 2.50−2.45 (m, 2H), 2.38 (s, 6H),

2.00−1.93 (m. 2H), 1.21 (t, 6H, J = 7.2 Hz). ^{13}C NMR ($CDCl_3$, 75 MHz) δ 172.9, 155.4, 155.4, 148.6, 145.5, 52.6, 46.4, 46.4, 36.5, 22.3, 18.8, 18.8, 10.7, 10.7. LRMS (FAB) m/z 281 (M + H$^+$). HRMS (FAB) calcd for $C_{14}H_{25}N_4O_2$ (M + H$^+$): 281.1972; found 281.1978.

*N^1-(5-(Benzyloxy)-4,6-dimethylpyrimidin-2-yl)-N^4,N^4-diethylbutane-1,4-diamine (**10a**).* To a solution of **9a** (13 mg, 0.04 mmol) in dry THF (2 mL) at 0 °C was added $LiAlH_4$ (13.3 mg, 0.35 mmol) portionwise. The mixture was stirred for 8 h at ambient temperature, cooled to 0 °C, and quenched by slow addition of Rochelle's solution followed by EtOAc. The organic phase was washed with water and brine, dried over $MgSO_4$, and concentrated *in vacuo*. Purification of the residue via flash column chromatography on silica gel (MeOH/CH_2Cl_2 = 1:1) afforded 5 mg (40%) of **10a** as a yellow oil. ^{1}H NMR (300 MHz, $CDCl_3$) δ 7.42−7.31 (m, 5H), 4.89 (bs, 1H), 4.71 (s, 2H), 3.37−3.36 (m, 2H), 2.55−2.45 (m, 6H), 2.28 (s, 6H), 1.56−1.51 (m, 4H), 1.01 (t, 6H, J = 7.1 Hz). LRMS (FAB) m/z 357 (M + H$^+$). ^{13}C NMR ($CDCl_3$, 100 MHz) δ 160.7, 160.7, 158.3, 142.4, 136.9, 128.6, 128.6, 128.3, 128.1, 128.1, 75.4, 52.7, 46.8, 46.8, 41.8, 28.0, 24.5, 19.1, 19.1, 11.7, 11.7. HRMS (FAB) calcd for $C_{21}H_{33}N_4O$ (M + H$^+$): 357.2649; found 357.2654.

*N^1,N^1-Diethyl-N^4-(5-methoxy-4,6-dimethylpyrimidin-2-yl)butane-1,4-diamine (**10b**).* Diamine **10b** was prepared by the procedure for **10a**, using **9b** (17 mg, 0.06 mmol) instead of **9a**. Purification of the residue via flash column chromatography on silica gel (MeOH/CH_2Cl_2 = 2:1) afforded 7.2 mg (44%) of **10b** as a yellow oil. ^{1}H NMR (300 MHz, CD_3OD) δ 3.67 (s, 3H), 3.38−3.34 (m, 2H), 2.65−2.52 (m, 6H), 2.28 (s, 6H), 1.58−1.55 (m, 4H), 1.05 (t, 6H, J = 7.1 Hz). ^{13}C NMR ($CDCl_3$, 75 MHz) δ 160.3, 160.3, 158.3, 143.7, 60.7, 52.7, 46.8, 46.8, 41.7, 28.0, 24.4, 18.7, 18.7, 11.6, 11.6. LRMS (FAB) m/z 281 (M + H$^+$). HRMS (FAB) calcd for $C_{15}H_{29}N_4O$ (M + H$^+$): 281.2336; found 281.2341.

*2-((4-(Diethylamino)butyl)amino)-4,6-dimethylpyrimidin-5-ol (**10c**).* Pyrimidol **10c** was prepared using the procedure for **9c**, using **10a** (7 mg, 0.02 mmol) instead of **9a**. Purification of the residue via flash column chromatography on silica gel (MeOH/CH_2Cl_2 = 3:1) afforded 4 mg (73%) of **10c** as a yellow oil. ^{1}H NMR (300 MHz, CD_3OD) δ 2.92−2.80 (m, 6H), 2.58−2.47 (m, 2H), 2.37 (s, 6H), 2.00−1.91 (m, 2H), 1.18 (t, 6H, J = 7.1 Hz). LRMS (FAB) m/z 267 (M + H$^+$). ^{13}C NMR ($CDCl_3$, 150 MHz) δ 157.1, 155.2, 155.2, 139.1, 52.6, 46.7, 46.7, 41.8, 28.0, 24.2, 18.7, 18.7, 11.4, 11.4. HRMS (FAB) calcd for $C_{14}H_{27}N_4O_2$ (M + H$^+$): 267.2179; found 281.2185.

*2,4-Dichloro-6-(1H-pyrrol-1-yl)pyrimidine (**14**).* To a solution of 4-amino-2,6-dichoropyrimidine (500 mg, 3.05 mmol) in acetic acid (5 mL) was added 2,5-dimethoxy-tetrahydrofuran (0.47 mL, 3.66 mmol). The reaction mixture was refluxed for 3 h and then diluted with EtOAc. The organic layer was washed with water and brine, dried over $MgSO_4$, and concentrated *in vacuo*. Purification of the residue via flash column chromatography on silica gel (EtOAc/*n*-hexane/CH_2Cl_2 = 1:40:5) afforded 540 mg (83%) of **14** as a white solid with a melting point of 78−80 °C. ^{1}H NMR (400 MHz, CD_3OD) δ 7.73−7.71 (m, 1H), 7.62 (s, 2H), 6.39 (s, 2H).

*2-Chloro-4,6-bis(4-chlorophenyl)pyrimidine (**15**).* To a solution of **11** (300 mg, 1.64 mmol) and 4-chlorophenylboronic acid (642 mg, 4.10 mmol) in THF (10 mL) was added Na_2CO_3 (867 mg, 8.18 mmol) in H_2O (10 mL) and $Pd(PPh_3)_4$ (95 mg, 0.08 mmol). The reaction mixture was refluxed for 4 h and diluted with EtOAc. The organic layer was washed with water and brine, dried over $MgSO_4$, and concentrated *in vacuo*. Purification of the residue via flash column chromatography on silica gel (EtOAc/*n*-hexane/CH_2Cl_2 = 1:40:5) afforded 305 mg (55%) of **15** as a white solid with a melting point of 163−165 °C. ^{1}H NMR (500 MHz, DMSO-d_6) δ 8.71 (s, 1H), 8.38 (d, 4H, J = 8.6 Hz), 7.67 (d, 4H, J = 8.6 Hz). LRMS (FAB) m/z 335 (M + H$^+$).

*2-Chloro-4-(4-chlorophenyl)-6-(piperidin-1-yl)pyrimidine (**16**).* To a solution of **11** (250 mg, 1.36 mmol) and 4-chlorophenylboronic acid (220 mg, 1.47 mmol) in glyme (10 mL) was added Na_2CO_3 (447 mg, 4.22 mmol) in H_2O (10 mL) and $Pd(PPh_3)_4$ (78 mg, 0.07 mmol). The reaction mixture was stirred at 70 °C for 24 h. The glyme was removed under reduced pressure, and the residue was diluted with EtOAc. The organic phase was washed with water and brine, dried over $MgSO_4$, and concentrated *in vacuo*. To a solution of the resulting white solid in EtOH (20 mL) was added piperidine (0.15 mL, 1.47 mmol). The reaction mixture was stirred for 5 h at ambient temperature and concentrated under reduced pressure. The residue was diluted with EtOAc. The EtOAc solution was washed with water and brine, dried over $MgSO_4$, and concentrated *in vacuo*. Purification of the residue via flash column chromatography on silica gel (EtOAc/*n*-hexane/CH_2Cl_2 = 1:20:1) afforded 138 mg (33%) of **16** as a white solid with a melting point of 147−150 °C. ^{1}H NMR (300 MHz, $CDCl_3$) δ 7.87 (d, 2H, J = 8.6 Hz), 7.40 (d, 2H, J = 8.6 Hz), 6.69 (s, 1H), 3.67 (bs, 4H), 1.75−1.60 (m, 6H). LRMS (FAB) m/z 308 (M + H$^+$).

*4-(2-Chloro-6-(4-chlorophenyl)pyrimidin-4-yl)morpholine (**17**).* Morpholine **17** was prepared from **11** (250 mg, 1.36 mmol) by the procedure for **16**, using morpholine instead of piperidine. Purification of the residue via flash column chromatography on silica gel (EtOAc/*n*-hexane = 1:6) afforded 165 mg (39%) of **17** as a white solid with a melting point of 197−200 °C. ^{1}H NMR (300 MHz, $CDCl_3$) δ 7.88 (d, 2H, J = 8.6 Hz), 7.41 (d, 2H, J = 8.4 Hz), 6.70 (s, 1H), 3.80−3.77 (m, 4H), 3.71−3.69 (m, 4H). LRMS (ESI) m/z 310 (M + H$^+$).

*2-Chloro-4-(4-chlorophenyl)-6-(4-methylpiperazin-1-yl)-pyrimidine (**18**).* Pyrimidine **18** was prepared from **11** (250 mg, 1.36 mmol) by the procedure for **16**, using 1-methyl piperazine instead of piperidine. Purification of the residue via flash column chromatography on silica gel (EtOAc/MeOH = 100:1) afforded 140 mg (32%) of **18** as yellow solid with a melting point of 120−122 °C. ^{1}H NMR (300 MHz, $CDCl_3$) δ 7.88 (d, 2H, J = 8.6 Hz), 7.41 (d, 2H, J = 8.6 Hz), 6.72 (s, 1H), 3.82 (bs, 4H), 2.61 (bs, 4H), 2.42 (s, 3H). LRMS (FAB) m/z 323 (M + H$^+$).

*2-Chloro-4-(4-chlorophenyl)-6-(1H-pyrrol-1-yl)pyrimidine (**19**).* To a solution of **14** (50 mg, 0.23 mmol) and 4-chlorophenylboronic acid (43 mg, 0.28 mmol) in THF (5 mL) was added Na_2CO_3 (86 mg, 0.55 mmol) in H_2O (5 mL) and $Pd(PPh_3)_4$ (13 mg, 0.011 mmol). The reaction mixture was refluxed for 10 h and diluted with EtOAc. The organic layer was washed with water and brine, dried over $MgSO_4$, and concentrated *in vacuo*. Purification of the residue via flash column chromatography on silica gel (EtOAc/*n*-hexane/CH_2Cl_2 = 1:40:1) afforded 38 mg (57%) of **19** as a white solid with a melting point of 136−142 °C. ^{1}H NMR (300 MHz, $CDCl_3$) δ 8.01 (d, 2H, J = 8.6 Hz), 7.57 (t, 2H, J = 2.3 Hz), 7.48 (d, 2H, J = 8.4 Hz), 7.42 (s, 1H), 6.41 (t, 2H, J = 2.3 Hz). LRMS (FAB) m/z 290 (M + H$^+$).

*2-Chloro-4-methyl-6-phenylpyrimidine (**20a**).* To a solution of **12** (100 mg, 0.61 mmol) and phenylboronic acid (89 mg, 0.73 mmol) in THF (5 mL) was added Na_2CO_3 (155 mg, 1.46 mmol) in H_2O (5 mL) and $Pd(PPh_3)_4$ (35 mg, 0.031 mmol). The reaction mixture was stirred refluxed for 4 h and diluted with EtOAc. The organic layer was washed with water and brine, dried over $MgSO_4$, and concentrated *in vacuo*. Purification of the residue via flash column chromatography on silica gel (EtOAc/*n*-hexane/CH_2Cl_2 = 1:20:1) afforded 126 mg (62%) of **20a** as a white solid with a melting point of 45−49 °C. ^{1}H NMR (300 MHz, CD_3OD) δ 8.16−8.13 (m, 2H), 7.84 (s, 1H), 7.55−7.49 (m, 3H), 2.56 (s, 3H). LRMS (FAB) m/z 205 (M + H$^+$).

*2-Chloro-4-(4-chlorophenyl)-6-methylpyrimidine (**20b**).* Pyrimidine **20b** was prepared from **12** (200 mg, 1.23 mmol) by the procedure for **20a**, using 4-chlorophenylboronic acid (211 mg, 1.35 mmol) instead of phenylboronic acid. Purification of the residue via flash column chromatography on silica gel (EtOAc/*n*-hexane/CH_2Cl_2 = 1:20:1) afforded 210 mg (71%) of **20b** as a white solid with a melting point of 118−121 °C. ^{1}H NMR (300 MHz, $CDCl_3$) δ 8.00 (d, 2H, J = 8.4 Hz), 7.47−7.44 (m, 3H), 2.58 (s, 3H). LRMS (FAB) m/z 239 (M + H$^+$).

*2-Chloro-4-(4-methoxyphenyl)-6-methylpyrimidine (**20c**).* Pyrimidine **20c** was prepared from **12** (100 mg, 0.61 mmol) by the procedure for **20a**, using 4-methoxyphenylboronic acid (102 mg, 0.67 mmol) instead of phenylboronic acid. Purification of the residue via flash column chromatography on silica gel (EtOAc/*n*-hexane/CH_2Cl_2 = 1:5:0.1) afforded 106 mg (73%) of **20c** as a white solid with a melting point of 66−68 °C. ^{1}H NMR (300 MHz, $CDCl_3$) δ 8.04 (d, 2H, J = 8.8 Hz), 7.41 (s, 1H), 6.98 (d, 2H, J = 8.8 Hz), 3.86 (s, 3H), 2.54 (s, 3H). LRMS (FAB) m/z 235 (M + H$^+$).

*4-(2-Chloro-6-methylpyrimidin-4-yl)phenol (**20d**).* Phenol **20d** was prepared from **12** (1.0 g, 6.13 mmol) by the procedure for **20a**, using 4-hydroxyphenylboronic acid (930 mg, 6.75 mmol) instead of phenylboronic acid. Purification of the residue via flash column chromatography on silica gel (EtOAc/*n*-hexane/CH_2Cl_2 = 1:3:0.1) afforded 825 mg (61%) of **20c** as a white solid with a melting point of 208−210 °C. ^{1}H NMR (300 MHz, $CDCl_3$) δ 7.98 (d, 2H, J = 8.6 Hz) 7.40 (s, 1H), 6.91 (d, 2H, J = 8.6 Hz), 2.54 (s, 3H). LRMS (FAB) m/z 221 (M + H$^+$).

*2-Chloro-4-(4-(cyclohexyloxy)phenyl)-6-methylpyrimidine (**21a**).* To a solution of **20d** (20 mg, 0.091 mmol) and triphenylphosphine (31 mg, 0.12 mmol) in THF (2 mL) was added cyclohexanol (12 mg, 0.12 mmol) and diisopropyl azodicarboxylate (24 μL, 0.12 mmol). The reaction mixture was stirred for 3 h at ambient temperature and quenched with H_2O. The reaction mixture was diluted with EtOAc. The organic layer was washed with water and brine, dried over $MgSO_4$, and concentrated *in vacuo*. Purification of the residue via flash column chromatography on silica gel (EtOAc/*n*-hexane = 1:5) afforded 18 mg (60%) of **21a** as a white solid with a melting point of 94−99 °C. ^{1}H NMR (300 MHz, $CDCl_3$) δ 7.99 (d, 2H, J = 8.3 Hz), 7.39 (s, 1H), 6.95 (d, 2H, J = 8.4 Hz), 4.36−4.30 (m, 1H), 2.53 (s, 3H), 2.10−1.89 (m, 2H), 1.80−1.75 (m, 2H), 1.58−1.28 (m, 6H). LRMS (FAB) m/z 303 (M + H$^+$).

*2-Chloro-4-(4-(2-cyclohexylethoxy)phenyl)-6-methylpyrimidine (**21b**).* Pyrimidine **21b** was prepared from **20d** (45 mg, 0.20 mmol) by the procedure for **21a**, using 2-cyclohexylethanol (34 mg, 0.27 mmol) instead of cyclohexanol. Purification of the residue via flash column chromatography on silica gel (EtOAc/*n*-hexane = 1:5) afforded 52 mg (78%) of **21b** as a white solid with a melting point of 79−83 °C. ^{1}H NMR (300 MHz, $CDCl_3$) δ 8.01 (d, 2H, J = 8.6 Hz), 7.39 (s, 1H), 6.95 (d, 2H, J = 8.6 Hz), 4.03 (t, 2H, J = 6.9 Hz), 2.52 (s, 3H), 1.74−1.65 (m, 6H), 1.51−1.40 (m, 1H), 1.26−1.19 (m, 4H), 1.01−0.93 (m, 2H). LRMS (FAB) m/z 331 (M + H$^+$).

*2-Chloro-4-methyl-6-(4-phenethoxyphenyl)pyrimidine (**21c**).* Pyrimidine **21c** was prepared from **20d** (30 mg, 0.14 mmol) by the procedure for **21a**, using phenethyl alcohol (20 mg, 0.16 mmol) instead of cyclohexanol. Purification of the residue via flash column chromatography on silica gel (EtOAc/*n*-hexane = 1:5) afforded 29 mg (64%) of **21c** as a white solid with a melting point of 96−99 °C. ^{1}H NMR (500 MHz, DMSO-d_6) δ 8.13 (d, 2H, J = 8.9 Hz), 7.94 (s, 1H), 7.35−7.30 (m, 4H), 7.24−7.23 (m, 1H), 7.10 (d, 2H, J = 8.9 Hz), 4.29 (t, 2H, J = 6.9 Hz), 3.01 (t, 2H, J = 6.9 Hz), 2.49 (s, 3H). LRMS (FAB) m/z 345 (M + H$^+$).

*2-Chloro-4-(4-((4-chlorobenzyl)oxy)phenyl)-6-methylpyrimidine (**21d**).* Pyrimidine **21d** was prepared from **20d** (30 mg, 0.14 mmol) by the procedure for **21a**, using 4-chlorobenzyl alcohol (23 mg, 0.16 mmol) instead of cyclohexanol. Purification of the residue via flash column chromatography on silica gel (EtOAc/*n*-hexane/CH_2Cl_2 = 1:6:0.5) afforded 32 mg (66%) of **21d** as yellow solid with a melting point of 166−168 °C. ^{1}H NMR (300 MHz, $CDCl_3$) δ 8.03 (d, 2H, J = 9.0 Hz), 7.41 (s, 1H), 7.46 (bs, 4H), 7.03 (d, 2H, J = 9.0 Hz), 5.09 (s, 2H), 2.54 (s, 3H). LRMS (FAB) m/z 345 (M + H$^+$).

*2-Chloro-4-(4-(4-chlorophenethoxy)phenyl)-6-methylpyrimidine (**21e**).* Pyrimidine **21e** was prepared from **20d** (30 mg, 0.14 mmol) by the procedure for **21a**, using 4-chlorophenylethanol (26 mg, 0.16 mmol) instead of cyclohexanol. Purification of the residue via flash column chromatography on silica gel (EtOAc/*n*-hexane = 1:6) afforded 32 mg (66%) of **21e** as a white solid with a melting point of 112−115 °C. ^{1}H NMR (300 MHz, CD_3OD) δ 8.08 (d, 2H, J = 9.0 Hz), 7.72 (s, 1H), 7.29 (bs, 4H), 7.02 (d, 2H, J = 9.0 Hz). LRMS (FAB) m/z 359 (M + H$^+$).

*2-Chloro-4-(4-(4-chlorophenoxy)phenyl)-6-methylpyrimidine (**21f**).* To a solution of **20d** (85 mg, 0.39 mmol), 4-chlorophenylboronic acid (180 mg, 1.15 mmol), and copper acetate (69 mg, 0.39 mmol) in the presence of 4 Å molecular sieves in CH_2Cl_2 (5 mL) was added triethylamine (0.25 mL, 1.79 mmol). The reaction mixture was vigorously stirred at ambient temperature for 24 h and filtered through a Celite pad. The filtrate was concentrated *in vacuo* and diluted with EtOAc. The organic layer was washed with saturated NH_4Cl solution and brine, dried over $MgSO_4$, and concentrated *in vacuo*. The residue was purified via flash column chromatography on silica gel (EtOAc/*n*-hexane/CH_2Cl_2 = 1:6:0.5) affording 32 mg (38%) of **20d** and 17 mg (13%) of **21f** as a white solid with a melting point of 129−132 °C. ^{1}H NMR (300 MHz, $CDCl_3$) δ 8.04 (d, 2H, J = 8.8 Hz), 7.43 (s, 1H), 7.34−7.31 (m, 2H), 7.04 (d, 2H, J = 8.8 Hz), 7.00−6.97 (m, 2H), 2.56 (s, 3H). LRMS (FAB) m/z 331 (M + H$^+$).

*2-Chloro-4-cyclohexyl-6-methylpyrimidine (**22**).* To a 0.5 M solution of cyclohexylzinc bromide in THF (3.0 mL, 1.50 mmol) was added 2,4-dichloro-6-methylpyrimidine **12** (245 mg, 1.50 mmol) and $Pd(PPh_3)_4$ (87 mg, 0.075 mmol) at ambient temperature. The reaction mixture was stirred, refluxed for 3 h, and diluted with EtOAc. The organic layer was washed with water and brine, dried over $MgSO_4$, and concentrated *in vacuo*. Purification of the residue via flash column chromatography on silica gel (EtOAc/*n*-hexane/CH_2Cl_2 = 1:20:0.5) afforded 270 mg (85%) of **22** as a white solid with a melting point of 77−81 °C. ^{1}H NMR (300 MHz, $CDCl_3$) δ 6.92 (s, 1H), 2.68−2.52 (m, 1H), 2.47 (s, 3H), 1.93−1.81 (m, 4H), 1.74−1.71 (m, 1H), 1.52−1.21 (m, 5H). LRMS (FAB) m/z 211 (M + H$^+$).

*2-Chloro-4-methyl-6-(piperidin-1-yl)pyrimidine (**23**).* To a solution of **12** (100 mg, 0.74 mmol) in EtOH (7 mL) was added piperidine (0.11 mL, 1.10 mmol). The reaction mixture was stirred for 1 h at ambient temperature and diluted with EtOAc. The organic layer was washed with water and brine, dried over $MgSO_4$, and concentrated *in vacuo*. Purification of the residue via flash column chromatography on silica gel (EtOAc/*n*-hexane = 1:7) afforded 93 mg (60%) of **23** as a white solid with a melting point of 67−72 °C. ^{1}H NMR (300 MHz, $CDCl_3$) δ 6.20 (s, 1H), 3.58 (bs, 4H), 2.29 (s, 3H), 1.69−1.55 (m, 6H). LRMS (FAB) m/z 212 (M + H$^+$).

*2-Chloro-6-methyl-N-phenylpyrimidin-4-amine (**24**).* Amine **24** was prepared from **12** (100 mg, 0.74 mmol) by the procedure for **23**, using aniline (0.1 mL, 1.10 mmol) instead of piperidine. Purification of the residue via flash column chromatography on silica gel (EtOAc/*n*-hexane = 1:4) afforded 50 mg (31%) of **24** as a white solid with a melting point of 117−120 °C. ^{1}H NMR (300 MHz, $CDCl_3$) δ 7.54 (d, 2H, J = 8.3 Hz), 7.37−7.31 (m, 2H), 7.13−7.08 (m, 1H), 2.30 (s, 3H). LRMS (FAB) m/z 220 (M + H$^+$).

*1-(4-(Naphthalen-2-yloxy)phenyl)ethanone (**26**).* To a solution of **25** (1.0 g, 7.24 mmol) and K_2CO_3 (3.0 g, 21.72 mmol) in dry DMF (20 mL) at ambient temperature was added 2-naphthol (1.5 g, 10.86 mmol). The reaction mixture was stirred for 24 h at 120 °C and diluted with EtOAc. The organic layer was washed with water and brine, dried over $MgSO_4$, and concentrated *in vacuo*. Purification of the residue via flash column chromatography on silica gel (EtOAc/*n*-hexane/CH_2Cl_2 = 1:20:0.5) afforded 1.7 g (91%) of **26** as a white solid with a melting point of 68−72 °C. ^{1}H NMR (300 MHz, CD_3OD) δ 8.02−8.00 (m, 2H), 7.94−7.85 (m, 2H), 7.79−7.76 (m, 1H), 7.51−7.41 (m, 3H), 7.24 (dd, 1H, J = 8.8, 2.4 Hz), 2.56 (s, 3H). LRMS (FAB) m/z 263 (M + H$^+$).

*1-(4-(Naphthalen-2-yloxy)phenyl)butane-1,3-dione (**27**).* To a solution of **26** (580 mg, 2.21 mmol), ethyl acetate (0.44 mL, 4.42 mmol), 18-crown-6 (6 mg, 0.023 mmol), and EtOH (1 drop) in THF (50 mL) was added 60% NaH in mineral oil (177 mg, 4.42 mmol) portionwise. The reaction mixture was refluxed for 4 h and concentrated under reduced pressure. The residue was diluted with EtOAc. The EtOAc solution was washed with water and brine, dried over $MgSO_4$, and concentrated *in vacuo*. Purification of the residue via flash column chromatography on silica gel (EtOAc/*n*-hexane/CH_2Cl_2 = 1:30:0.5) afforded 525 mg (78%) of **27** as yellow solid with a melting point of 102−105 °C. ^{1}H NMR (300 MHz, CD_3OD) δ 8.00−7.86 (m, 4H), 7.78 (d, 1H, J = 7.3 Hz), 7.51−7.44 (m, 3H), 7.26 (dd, 1H J = 8.8, 2.4 Hz), 7.10−7.05 (m, 2H), 6.33 (s, 1H), 2.16 (s, 3H).

*2-Chloro-4-methyl-6-(4-(naphthalen-2-yloxy)phenyl)pyrimidine (**28**).* To a solution of **27** (420 mg, 1.38 mmol) in EtOH (7 mL) was added urea (133 mg, 2.21 mmol) and *c*-HCl (0.14 mL, 1.66 mmol). The reaction mixture was stirred, refluxed for 40 h, and cooled to ambient temperature. Et_2O (50 mL) was slowly added to reaction mixture. After filtration of the reaction mixture, the resulting white solid was used for next reaction without further purification. A suspension of the white solid in $POCl_3$ (5 mL) was stirred at reflux condition for 5 h and concentrated *in vacuo*. The residue was diluted

with CH_2Cl_2, and saturated $NaHCO_3$ solution was added dropwise at 0 °C. The organic layer was washed with water and brine, dried over $MgSO_4$, and concentrated *in vacuo*. Purification of the residue via flash column chromatography on silica gel (EtOAc/*n*-hexane/CH_2Cl_2 = 1:20:0.5) afforded 153 mg (32%) of **28** as a white solid with a melting point of 142−144 °C. ^{1}H NMR (300 MHz, $CDCl_3$) δ 8.09−8.03 (m, 2H), 7.88−7.83 (m, 2H), 7.74−7.72 (m, 1H), 7.51−7.42 (m, 4H), 7.28−7.25 (m, 1H), 7.15−7.10 (m, 2H), 2.57 (s, 3H). LRMS (FAB) *m*/*z* 347 (M + H$^+$).

*N,N-Diethyl-2-(4-nitrophenoxy)ethanamine (**30a**).* To a solution of 4-nitrophenol **29a** (200 mg, 1.44 mmol) and triphenylphosphine (490 mg, 1.87 mmol) in THF (10 mL) was added *N,N*-diethyl ethanolamine (0.25 mL, 1.87 mmol) and diisopropyl azodicarboxylate (0.37 mL, 1.87 mmol). The reaction mixture was stirred for 3 h at ambient temperature and quenched with H_2O. The reaction mixture was diluted with EtOAc. The organic layer was washed with water and brine, dried over $MgSO_4$, and concentrated *in vacuo*. Purification of the residue via flash column chromatography on silica gel (MeOH/CH_2Cl_2 = 1:20) afforded 278 mg (81%) of **30a** as a yellow oil. ^{1}H NMR (300 MHz, $CDCl_3$) δ 8.16 (d, 2H, *J* = 9.3 Hz), 6.93 (d, 2H, *J* = 9.3 Hz), 4.11 (t, 2H, *J* = 6.0 Hz), 2.88 (t, 2H, *J* = 6.0 Hz), 2.63 (q, 4H, *J* = 7.1 Hz), 1.05 (t, 6H, *J* = 7.1 Hz). LRMS (FAB) *m*/*z* 239 (M + H$^+$).

*N,N-Diethyl-2-(3-nitrophenoxy)ethanamine (**30b**).* Amine **30b** was prepared by the procedure for **30a** using **29b** (200 mg, 1.44 mmol) instead of **29a**. Purification of the residue via flash column chromatography on silica gel (MeOH/CH_2Cl_2 = 1:20) afforded 285 mg (83%) of **30b** as a yellow oil. ^{1}H NMR (300 MHz, $CDCl_3$) δ 7.81−7.78 (m, 1H), 7.72 (t, 1H, *J* = 2.3 Hz), 7.40 (t, 1H, *J* = 11.2 Hz), 7.23−7.20 (m, 1H), 4.12 (t, 2H, *J* = 5.9 Hz), 2.91 (t, 2H, *J* = 6.0 Hz), 2.65 (q, 4H, *J* = 7.1 Hz), 1.08 (t, 6H, *J* = 7.1 Hz). LRMS (FAB) *m*/*z* 239 (M + H$^+$).

*N,N-Diethyl-2-(2-nitrophenoxy)ethanamine (**30c**).* Amine **30c** was prepared by the procedure for **30a**, using **29c** (300 mg, 2.16 mmol) instead of **29a**. Purification of the residue via flash column chromatography on silica gel (MeOH/CH_2Cl_2 = 1:20) afforded 420 mg (82%) of **30c** as a yellow oil. ^{1}H NMR (300 MHz, $CDCl_3$) δ 7.80 (dd, 1H, *J* = 1.7, 8.0 Hz), 7.52−7.46 (m, 1H), 7.08−6.97 (m, 2H), 4.16 (t, 2H, *J* = 6.1 Hz), 2.92 (t, 2H, *J* = 6.1 Hz), 2.63 (t, 4H, *J* = 7.1 Hz), 1.05 (t, 6H, J = 7.1 Hz). LRMS (ESI) *m*/*z* 239 (M + H$^+$).

*2-(4-Bromophenoxy)-N,N-diethylethanamine (**30d**).* Amine **30d** was prepared by the procedure for **30a**, using 4-bromophenol **30d** (890 mg, 5.14 mmol) instead of **30a**. Purification of the residue via flash column chromatography on silica gel (MeOH/CH_2Cl_2 = 1:20) afforded 1.22 g (87%) of **30d** as yellow oil. ^{1}H NMR (300 MHz, $CDCl_3$) δ 7.36−7.32 (m, 2H), 6.78−6.73 (m, 2H), 3.98 (t, 2H, *J* = 6.3 Hz), 2.83 (t, 2H, *J* = 6.2 Hz), 2.60 (q, 4H, *J* = 7.1 Hz), 1.04 (t, 6H, *J* = 7.1 Hz). LRMS (FAB) *m*/*z* 272 (M + H$^+$).

*4-(2-(Diethylamino)ethoxy)aniline (**31a**).* To a solution of **30a** (100 mg, 0.42 mmol) in EtOH (5 mL) was added $SnCl_2 \cdot 2H_2O$ (473 mg, 2.10 mmol). The reaction mixture was stirred, refluxed for 3 h, and concentrated *in vacuo*. The residue was diluted with EtOAc and saturated $NaHCO_3$ solution was added. The mixture was filtered using a Celite pad. The organic phase was washed with water and brine, dried over $MgSO_4$, and concentrated *in vacuo*. Purification of the residue via flash column chromatography on silica gel (MeOH/CH_2Cl_2 = 1:10) afforded 77 mg (88%) of **31a** as a brown oil. ^{1}H NMR (300 MHz, CD_3OD) δ 6.75−6.67 (m, 4H), 3.99 (t, 2H, *J* = 5.9 Hz), 2.84 (t, 2H, *J* = 5.8 Hz), 2.65 (q, 4H, *J* = 7.2 Hz), 1.07 (t, 6H, *J* = 7.1 Hz). LRMS (FAB) *m*/*z* 209 (M + H$^+$).

*3-(2-(Diethylamino)ethoxy)aniline (**31b**).* Aniline **31b** was prepared by the procedure for **31a**, using **30b** (1.9 g, 7.70 mmol) instead of **30a**. Purification of the residue via flash column chromatography on silica gel (MeOH/CH_2Cl_2 = 1:10) afforded 1.3 g (81%) of **31b** as a brown oil. ^{1}H NMR (300 MHz, $CDCl_3$) δ 7.02 (t, 1H, *J* = 8.0 Hz), 6.31−6.22 (m, 3H), 4.02 (t, 2H, *J* = 6.2 Hz), 3.62 (bs, 2H), 2.89 (t, 2H, *J* = 6.2 Hz), 2.65 (q, 4H, *J* = 7.1 Hz), 1.07 (t, 6H, *J* = 7.1 Hz). LRMS (FAB) *m*/*z* 209 (M + H$^+$).

*2-(2-(Diethylamino)ethoxy)aniline (**31c**).* Aniline **31c** was prepared by the procedure for **31a**, using **30c** (320 mg, 1.34 mmol) instead of **30a**. Purification of the residue via flash column chromatography on silica gel (MeOH/CH_2Cl_2 = 1:10) afforded 244 mg (87%) of **31c** as a brown oil. ^{1}H NMR (300 MHz, $CDCl_3$) δ 6.80−6.75 (m, 2H), 6.71−6.67 (m, 2H), 4.06 (t, 2H, *J* = 6.0 Hz), 3.65 (bs, 2H), 2.89 (t, 2H, *J* = 6.1 Hz), 2.64 (q, 4H, *J* = 7.1 Hz), 1.06 (t, 6H, *J* = 7.1 Hz). LRMS (FAB) *m*/*z* 209 (M + H$^+$).

*5-(Benzyloxy)-N-(4-(2-(diethylamino)ethoxy)phenyl)-4,6-dimethylpyrimidin-2-amine (**32**).* To a solution of **5a** (100 mg, 0.44 mmol), **30d** (119 mg, 0.44 mmol), and 4,5-bis(diphenylphosphino)-9,9-dimethylxanthene (xantphos) (26 mg, 0.04 mmol) in toluene (10 mL) was added $CsCO_3$ (215 mg, 0.66 mmol) and $Pd(OAc)_2$ (5 mg, 0.02 mmol). The reaction mixture was stirred refluxed for 24 h and quenched with H_2O. The reaction mixture was diluted with EtOAc. The mixture was washed with water and brine, dried over $MgSO_4$, and concentrated *in vacuo*. Purification of the residue via flash column chromatography on silica gel (MeOH/CH_2Cl_2 = 1:15) afforded 40 mg (22%) of **32** as colorless oil. ^{1}H NMR (300 MHz, CD_3OD) δ 7.56−7.51 (m, 2H), 7.45−7.36 (m, 5H), 6.90−6.85 (m, 2H), 4.82 (s, 2H), 4.11 (t, 2H, *J* = 5.5 Hz), 3.00 (t, 2H, *J* = 5.5 Hz), 2.78 (q, 4H, *J* = 7.1 Hz), 2.29 (s, 6H), 1.14 (t, 6H, *J* = 7.1 Hz). ^{13}C NMR ($CDCl_3$, 150 MHz) δ 160.9, 160.9, 155.6, 146.7, 144.6, 143.5, 136.7, 128.7, 128.7, 128.4, 128.2, 128.2, 120.3, 120.3, 114.9, 114.9, 75.5, 66.9, 51.8, 47.8, 47.8, 19.1, 19.1, 11.8, 11.8. LRMS (FAB) *m*/*z* 421 (M + H$^+$). HRMS (FAB) calcd for $C_{25}H_{33}N_4O_2$ (M + H$^+$): 421.2598; found 421.2604.

*2-((4-(2-(Diethylamino)ethoxy)phenyl)amino)-4,6-dimethylpyrimidin-5-ol (**33**).* A suspension of **32** (20 mg, 0.05 mmol) and 20% $Pd(OH)_2$ (2 mg) in MeOH (5 mL) was stirred under H_2 for 10 h at ambient temperature. The reaction mixture was filtered through a Celite pad and concentrated *in vacuo*. Purification of the residue via flash column chromatography on silica gel (MeOH/CH_2Cl_2 = 7:1) afforded 13 mg (83%) of **33** as a colorless oil. ^{1}H NMR (300 MHz, CD_3OD) δ 7.53−7.48 (m, 2H), 6.89−6.85 (m, 2H), 4.12 (t, 2H, *J* = 5.5 Hz), 3.07 (t, 2H, *J* = 5.5 Hz), 2.84 (q, 4H, *J* = 7.3 Hz), 2.32 (s, 6H), 1.16 (t, 6H, *J* = 7.2 Hz). LRMS (FAB) *m*/*z* 331 (M + H$^+$). ^{13}C NMR ($CDCl_3$, 75 MHz) δ 170.9, 154.7, 154.7, 153.9, 140.4, 134.2, 119.8, 119.8, 114.8, 114.8, 65.9, 51.5, 47.4, 47.4, 18.8, 18.8, 10.8, 10.8. HRMS (FAB) calcd for $C_{18}H_{27}N_4O_2$ (M + H$^+$): 331.2129; found 331.2134.

General Synthetic Procedure for the N-Aryl Pyrimidine Analogs. To a solution of 2-chloropyrimidine intermediates (1 equiv) and aniline (1 equiv) in *n*-BuOH (1 mL) was added catalytic amount of 4 N hydrogen chloride in dioxane. The reaction mixture was stirred for 1 h at 160 °C under microwave irradiation and concentrated *in vacuo*. The residue was diluted with EtOAc and saturated $NaHCO_3$ solution. The organic layer was washed with water and brine, dried over $MgSO_4$, and concentrated *in vacuo*. Purification of the residue via flash column chromatography on silica gel (MeOH/CH_2Cl_2 = 1:10−1:20) afforded the corresponding *N*-aryl pyrimidine analog.

*N-(4-(2-(Diethylamino)ethoxy)phenyl)-4,6-dimethylpyrimidin-2-amine (**34**).* Chloropyrimidine **13** (20 mg, 0.14 mmol) afforded 18 mg of amine **34** (41%) as a colorless oil. ^{1}H NMR (300 MHz, CD_3OD) δ 7.55−7.52 (m, 2H), 6.89−6.86 (m, 2H), 6.52 (s, 1H), 4.07 (t, 2H, *J* = 5.8 Hz), 2.92 (t, 2H, *J* = 5.7 Hz), 2.70 (q, 4H, *J* = 7.3 Hz), 2.30 (s, 6H), 1.10 (t, 6H, *J* = 7.1 Hz). LRMS (FAB) *m*/*z* 315 (M + H$^+$). ^{13}C NMR ($CDCl_3$, 150 MHz) δ 167.5, 167.5, 160.0, 154.2, 133.2, 120.7, 220.6, 114.9, 114.9, 111.2, 66.7, 51.8, 47.8, 47.8, 23.9, 23.9, 11.7, 11.7. HRMS (FAB) calcd for $C_{18}H_{27}N_4O$ (M + H$^+$): 315.2179; found 315.2184.

*N-(3-(2-(Diethylamino)ethoxy)phenyl)-4,6-dimethylpyrimidin-2-amine (**35**).* Chloropyrimidine **13** (20 mg, 0.14 mmol) afforded 18 mg of amine **35** (41%) as a colorless oil. ^{1}H NMR (300 MHz, CD_3OD) δ 7.56−7.55 (m, 1H), 7.18−7.14 (m, 2H), 6.57−6.53 (m, 2H), 4.11 (t, 2H, *J* = 5.7 Hz), 2.98 (t, 2H, *J* = 5.7 Hz), 2.74 (q, 4H, *J* = 7.1 Hz), 2.33 (s, 6H), 1.11 (t, 6H, *J* = 7.1 Hz). ^{13}C NMR ($CDCl_3$, 100 MHz) δ 167.5, 167.5, 159.7, 159.3, 141.2, 129.5, 111.7, 111.3, 108.0, 105.3, 65.9, 51.6, 47.7, 47.7, 23.9, 23.9, 11.5, 11.5. LRMS (FAB) *m*/*z* 315 (M + H$^+$). HRMS (FAB) calcd for $C_{18}H_{27}N_4O$ (M + H$^+$): 315.2179; found 315.2184.

*4-Cyclohexyl-N-(4-(2-(diethylamino)ethoxy)phenyl)-6-methylpyrimidin-2-amine (**36**).* Chloropyrimidine **22** (30 mg, 0.14 mmol)

afforded 27 mg of amine **36** (51%) as a brown oil. ^{1}H NMR (500 MHz, $CDCl_3$) δ 7.54 (d, 2H, J = 8.9 Hz), 6.89 (s, 1H), 6.85 (d, 2H, J = 8.9 Hz), 6.41 (s, 1H), 4.05 (t, 2H, J = 6.2 Hz), 2.89 (t, 2H, J = 6.2 Hz), 2.66 (q, 4H, J = 7.0 Hz), 2.46 (td, 1H, J = 11.6, 3.3 Hz), 2.33 (s, 3H), 1.90 (d, 2H, J = 11.7 Hz), 1.84−1.81 (m, 2H), 1.72 (d, 1H, J = 12.7 Hz), 1.51−1.20 (m, 5H), 1.08 (t, 6H, J = 7.1 Hz). ^{13}C NMR ($CDCl_3$, 100 MHz) δ 175.4, 167.5, 159.8, 153.9, 133.6, 120.3, 120.3, 114.8, 114.8, 108.9, 66.4, 51.6, 47.7, 47.7, 45.9, 32.0, 32.0, 26.3, 26.3, 26.0, 24.1, 11.5, 11.5. LRMS (FAB) m/z 383 (M + H$^+$). HRMS (FAB) calcd for $C_{23}H_{35}N_4O$ (M + H$^+$): 383.2805; found 383.2811.

*N-(4-(2-(Diethylamino)ethoxy)phenyl)-4-methyl-6-(piperidin-1-yl)pyrimidin-2-amine (**37**).* Chloropyrimidine **23** (25 mg, 0.12 mmol) afforded 14 mg of amine **37** (30%) as a colorless oil. ^{1}H NMR (300 MHz, $CDCl_3$) δ 7.46−7.43 (m, 2H), 6.85−6.80 (m, 2H), 5.84 (s, 1H), 4.03 (t, 2H, J = 6.4 Hz), 3.58−3.54 (m, 4H), 2.86 (t, 2H, J = 6.2 Hz), 2.64 (q, 4H, J = 7.1 Hz), 2.23 (s, 3H), 1.66−1.58 (m, 6H), 1.06 (t, 6H, J = 7.1 Hz). ^{13}C NMR ($CDCl_3$, 75 MHz) δ 187.3, 181.8, 180.1, 162.6, 137.4, 121.1, 121.1, 114.6, 114.6, 93.0, 66.5, 51.7, 47.7, 47.7, 45.5, 45.5, 29.7, 25.6, 25.6, 24.7, 11.6, 11.6. LRMS (FAB) m/z 384 (M + H$^+$). HRMS (FAB) calcd for $C_{22}H_{34}N_5O$ (M + H$^+$): 384.2758; found 384.2763.

*N^2-(4-(2-(Diethylamino)ethoxy)phenyl)-6-methyl-N^4-phenylpyrimidine-2,4-diamine (**38**).* Chloropyrimidine **24** (20 mg, 0.091 mmol) afforded 14 mg (39%) of diamine **38** as a yellow oil. ^{1}H NMR (300 MHz, CD_3OD) δ 7.57−7.48 (m, 4H), 7.27−7.22 (m, 2H), 7.01−6.97 (m, 1H), 6.91−6.87 (m, 2H), 6.03 (s, 1H), 4.15 (t, 2H, J = 5.5 Hz), 3.11 (t, 2H, J = 5.4 Hz), 2.87 (q, 4H, J = 7.3 Hz), 2.21 (s, 3H), 1.18 (t, 6H, J = 7.2 Hz). ^{13}C NMR ($CDCl_3$, 75 MHz) δ 166.9, 161.6, 160.1, 154.4, 138.7, 133.0, 129.1, 129.1, 124.0, 122.1, 122.1, 121.6, 121.6, 114.6, 114.6, 94.7, 66.7, 51.7, 47.7, 47.7, 24.0, 11.8, 11.8. LRMS (FAB) m/z 392 (M + H$^+$). HRMS (FAB) calcd for $C_{23}H_{30}N_5O$ (M + H$^+$): 392.2445; found 392.2456.

*N-(4-(2-(Diethylamino)ethoxy)phenyl)-4-methyl-6-phenylpyrimidin-2-amine (**39**).* Chloropyrimidine **20a** (25 mg, 0.12 mmol) afforded 13 mg (29%) of amine **39** as a yellow oil. ^{1}H NMR (300 MHz, CD_3OD) δ 8.11−8.08 (m, 2H), 7.67−7.63 (m, 2H), 7.48−7.46 (m, 3H), 7.14 (s, 1H), 6.93−6.90 (m, 2H), 4.11 (t, 2H, J = 5.6 Hz), 2.98 (t, 2H, J = 5.6 Hz), 2.76 (q, 4H, J = 7.1 Hz), 2.42 (s, 3H), 1.13 (t, 6H, J = 7.2 Hz). ^{13}C NMR ($CDCl_3$, 75 MHz) δ 186.5, 164.6, 160.3, 154.3, 137.4, 133.1, 130.4, 128.7, 128.7, 127.0, 127.0, 120.9, 120.9, 114.8, 114.8, 107.5, 66.8, 51.7, 47.7, 47.7, 24.3, 11.8, 11.8. LRMS (FAB) m/z 377 (M + H$^+$). HRMS (FAB) calcd for $C_{23}H_{29}N_4O$ (M + H$^+$): 377.2336; found 377.2338.

*N-(4-(2-(Diethylamino)ethoxy)phenyl)-4-(4-methoxyphenyl)-6-methylpyrimidin-2-amine (**40**).* Chloropyrimidine **20c** (20 mg, 0.09 mmol) afforded 12 mg (35%) of amine **40** as a colorless oil. ^{1}H NMR (300 MHz, CD_3OD) δ 8.08−8.03 (m, 2H), 7.66−7.60 (m, 2H), 7.07 (s, 1H), 7.03−6.98 (m, 2H), 6.94−6.88 (m, 2H), 4.09 (t, 2H, J = 5.7 Hz), 3.84 (s, 3H), 2.95 (t, 2H, J = 5.7 Hz), 2.73 (q, 4H, J = 7.2 Hz), 2.39 (s, 3H), 1.12 (t, 6H, J = 7.2 Hz). ^{13}C NMR (CD_3OD, 75 MHz) δ 170.1, 166.3, 163.9, 162.4, 156.0, 135.9, 131.5, 130.2, 130.2, 122.9, 122.9, 116.2, 116.2, 115.6, 115.6, 107.7, 67.4, 56.4, 53.2, 49.1, 49.1, 24.6, 11.7, 11.7. LRMS (FAB) m/z 407 (M + H$^+$). HRMS (FAB) calcd for $C_{24}H_{31}N_4O_2$ (M + H$^+$): 407.2442; found 407.2459.

*N-(3-(2-(Diethylamino)ethoxy)phenyl)-4-(4-methoxyphenyl)-6-methylpyrimidin-2-amine (**41**).* Chloropyrimidine **20c** (20 mg, 0.09 mmol) afforded 12 mg (35%) of amine **41** as a colorless oil. ^{1}H NMR (300 MHz, CD_3OD) δ 8.11−8.06 (m, 2H), 7.71−7.70 (m, 1H), 7.21−7.18 (m, 2H), 7.12 (s, 1H), 7.03−6.98 (m, 2H), 6.58−6.54 (m, 1H), 4.14 (t, 2H, J = 5.6 Hz), 3.85 (s, 3H), 3.00 (t, 2H, J = 5.6 Hz), 2.75 (q, 4H, J = 7.1 Hz), 2.42 (s, 3H), 1.12 (t, 6H, J = 7.2 Hz). ^{13}C NMR ($CDCl_3$, 75 MHz) 168.1, 164.1, 161.7, 159.9, 159.4, 141.3, 129.7, 129.4, 128.6, 128.6, 114.1, 114.1, 111.2, 108.2, 107.2, 105.1, 66.4, 55.3, 51.6, 47.8, 47.8, 24.3, 11.8, 11.8. LRMS (FAB) m/z 407 (M + H$^+$). HRMS (FAB) calcd for $C_{24}H_{31}N_4O_2$ (M + H$^+$): 407.2442; found 407.2447.

*4-(4-Chlorophenyl)-N-(4-(2-(diethylamino)ethoxy)phenyl)-6-methylpyrimidin-2-amine (**42**).* Chloropyrimidine **20b** (15 mg, 0.06 mmol) afforded 8 mg (31%) of amine **42** as a colorless oil. ^{1}H NMR (300 MHz, CD_3OD) δ 8.10−8.07 (m, 2H), 7.64−7.61 (m, 2H), 7.49−7.46 (m, 2H), 7.13 (s, 1H), 6.93−6.90 (m, 2H), 4.11 (t, 2H, J = 5.7 Hz), 2.97 (t, 2H, J = 5.7 Hz), 2.74 (q, 4H, J = 7.1 Hz), 2.42 (s, 3H), 1.13 (t, 6H, J = 7.1 Hz). ^{13}C NMR ($CDCl_3$, 75 MHz) δ 168.8, 163.4, 160.4, 154.6, 136.6, 135.9, 133.0, 129.0, 129.0, 128.4, 128.4, 121.0, 121.0, 114.9, 114.9, 107.3, 66.9, 51.9, 47.8, 47.8, 24.3, 11.8, 11.8. LRMS (FAB) m/z 411 (M + H$^+$). HRMS (FAB) calcd for $C_{23}H_{28}ClN_4O$ (M + H$^+$): 411.1946; found 411.1952.

*4-(4-Chlorophenyl)-N-(3-(2-(diethylamino)ethoxy)phenyl)-6-methylpyrimidin-2-amine (**43**).* Chloropyrimidine **20b** (15 mg, 0.06 mmol) afforded 9 mg (35%) of amine **43** as a colorless oil. ^{1}H NMR (300 MHz, CD_3OD) δ 8.13−8.10 (m, 2H), 7.68 (m, 1H), 7.50−7.47 (m, 2H), 7.19−7.18 (m, 3H), 6.56−6.55 (m, 1H), 4.12 (t, 2H, J = 5.7 Hz), 2.96 (t, 2H, J = 5.7 Hz), 2.71 (q, 4H, J = 7.2 Hz), 2.45 (s, 3H), 1.11 (t, 6H, J = 7.2 Hz). ^{13}C NMR ($CDCl_3$, 75 MHz) δ 168.8, 163.4, 160.0, 151.9, 141.0, 141.0, 135.8, 129.5, 129.0, 129.0, 128.4, 128.4, 111.2, 108.5, 107.8, 105.3, 66.5, 51.7, 47.8, 47.8, 24.4, 11.9, 11.9. LRMS (FAB) m/z 411 (M + H$^+$). HRMS (FAB) calcd for $C_{23}H_{28}ClN_4O$ (M + H$^+$): 411.1946; found 411.1953.

*4-(4-Chlorophenyl)-N-(2-(2-(diethylamino)ethoxy)phenyl)-6-methylpyrimidin-2-amine (**44**).* **20b** (15 mg, 0.06 mmol) afforded 9 mg (35%) of amine **44** as a colorless oil. ^{1}H NMR (300 MHz, CD_3OD) δ 8.50−8.47 (m, 1H), 8.10 (d, 2H, J = 8.6 Hz), 7.49 (d, 2H, J = 8.8 Hz), 7.21 (s, 1H), 7.05−6.95 (m, 3H), 4.22 (t, 2H, J = 5.6 Hz), 3.06 (t, 2H, J = 5.6 Hz), 2.78 (q, 4H, J = 7.2 Hz), 2.45 (s, 3H), 1.15 (t, 6H, J = 7.1 Hz). ^{13}C NMR ($CDCl_3$, 125 MHz) 168.7, 163.4, 163.3, 154.6, 140.1, 136.5, 139.5, 128.9, 128.9, 128.4, 128.4, 121.4, 121.3, 118.7, 112.2, 107.5, 67.9, 51.7, 47.8, 47.8, 24.4, 11.7, 11.7. LRMS (FAB) m/z 411 (M + H$^+$). HRMS (FAB) calcd for $C_{23}H_{28}ClN_4O$ (M + H$^+$): 411.1946; found 411.1957.

*4-(4-(4-Chlorophenoxy)phenyl)-N-(4-(2-(diethylamino)ethoxy)-phenyl)-6-methylpyrimidin-2-amine (**45**).* Chloropyrimidine **21f** (10 mg, 0.03 mmol) afforded 6 mg (41%) of amine **45** as a yellow oil. ^{1}H NMR (300 MHz, CD_3OD) δ 8.12−8.09 (m, 2H), 7.64−7.59 (m, 2H), 7.39−7.34 (m, 2H), 7.09 (s, 1H), 7.06−7.00 (m, 4H), 6.91−6.88 (m, 2H), 4.07 (t, 2H, J = 5.7 Hz), 2.93 (t, 2H, J = 5.7 Hz), 2.70 (q, 4H, J = 7.2 Hz), 2.40 (s, 3H), 1.10 (t, 6H, J = 7.2 Hz). LRMS (FAB) m/z 503 (M + H$^+$). ^{13}C NMR (CD_3OD, 75 MHz) δ 170.7, 166.0, 162.7, 161.6, 157.5, 156.3, 136.0, 133.7, 131.8, 131.8, 130.9, 130.9, 130.9, 123.2, 123.2, 122.7, 122.7, 120.2, 120.2, 116.5, 116.5, 108.3, 67.8, 53.5, 49.4, 49.4, 24.9, 12.1, 12.1. HRMS (FAB) calcd for $C_{29}H_{32}ClN_4O_2$ (M + H$^+$): 503.2208; found 503.2214.

*4-(4-((4-Chlorobenzyl)oxy)phenyl)-N-(4-(2-(diethylamino)-ethoxy)phenyl)-6-methylpyrimidin-2-amine (**46**).* Chloropyrimidine **21d** (10 mg, 0.03 mmol) afforded 6 mg (40%) of amine **46** as a yellow oil. ^{1}H NMR (300 MHz, CD_3OD) δ 8.05 (d, 2H, J = 9.0 Hz), 7.62 (d, 2H, J = 9.2 Hz), 7.44−7.35 (m, 4H), 7.07−7.04 (m, 3H), 6.90 (d, 2H, J = 9.2 Hz), 5.10 (s, 2H), 4.08 (t, 2H, J = 5.7 Hz), 2.93 (t, 2H, J = 5.7 Hz), 2.71 (q, 4H, J = 7.1 Hz), 2.39 (s, 3H), 1.11 (t, 6H, J = 7.2 Hz). ^{13}C NMR (CD_3OD, 125 MHz) δ 170.5, 166.5, 163.0, 162.7, 156.3, 138.1, 136.3, 135.6, 132.2, 131.0, 131.0, 130.6, 130.6, 130.5, 130.5, 123.2, 123.2, 116.8, 116.8, 116.5, 116.5, 108.1, 71.1, 67.1, 53.5, 49.5, 49.5, 24.9, 12.0, 12.0. LRMS (FAB) m/z 517 (M + H$^+$). HRMS (FAB) calcd for $C_{30}H_{34}ClN_4O_2$ (M + H$^+$): 517.2365; found 517.2370.

*4-(4-(4-Chlorophenethoxy)phenyl)-N-(4-(2-(diethylamino)-ethoxy)phenyl)-6-methylpyrimidin-2-amine (**47**).* Chloropyrimidine **21e** (20 mg, 0.06 mmol) afforded 16 mg (54%) of amine **47** as a yellow oil. ^{1}H NMR (300 MHz, CD_3OD) δ 8.02 (d, 2H, J = 9.0 Hz), 7.63 (d, 2H, J = 9.2 Hz), 7.28 (bs, 4H), 7.04 (s, 1H), 6.96 (d, 2H, J = 9.0 Hz), 6.90 (d, 2H, J = 9.0 Hz), 4.21 (t, 2H, J = 6.7 Hz), 4.08 (t, 2H, J = 5.7 Hz), 4.05 (t, 2H, J = 6.6 Hz), 2.95 (t, 2H, J = 5.7 Hz), 2.73 (q, 4H, J = 7.2 Hz), 2.38 (s, 3H), 1.11 (t, 6H, J = 7.2 Hz). ^{13}C NMR (CD_3OD, 75 MHz) δ 170.4, 166.5, 163.2, 162.6, 156.2, 139.5, 136.2, 134.1, 132.5, 132.5, 131.9, 130.6, 130.6, 130.3, 130.3, 123.2, 123.2, 116.5, 116.5, 116.5, 116.5, 108.0, 70.4, 67.6, 53.5, 49.4, 49.4, 36.7, 24.9, 12.0, 12.0. LRMS (FAB) m/z 531 (M + H$^+$). HRMS (FAB) calcd for $C_{31}H_{36}ClN_4O_2$ (M + H$^+$): 531.2521; found 531.2527.

*N-(4-(2-(Diethylamino)ethoxy)phenyl)-4-methyl-6-(4-phenethoxyphenyl)pyrimidin-2-amine (**48**).* Chloropyrimidine **21c** (27 mg, 0.08 mmol) afforded 15 mg (36%) of amine **48** as a yellow oil. ^{1}H NMR (300 MHz, CD_3OD) δ 7.95−7.92 (m, 2H), 7.56−7.53 (m,

dx.doi.org/10.1021/jm300172z | J. Med. Chem. 2012, 55, 9120−9135

2H), 7.21−7.16 (m, 4H), 7.15−7.07 (m, 1H), 6.96 (s, 1H), 6.89−6.85 (m, 2H), 6.83−6.80 (m, 2H), 4.13 (t, 2H, J = 6.9 Hz), 4.00 (t, 2H, J = 5.6 Hz), 2.98 (t, 2H, J = 6.8 Hz), 2.87 (t, 2H, J = 5.6 Hz), 2.65 (q, 4H, J = 7.1 Hz), 1.03 (t, 6H, J = 7.1 Hz). ^{13}C NMR (CD_3OD, 125 MHz) δ 170.3, 166.5, 163.3, 162.6, 156.2, 140.5, 136.2, 131.8, 130.9, 130.9, 130.5, 130.5, 130.3, 130.3, 128.3, 123.2, 123.2, 116.5, 116.5, 116.5, 116.5, 108.0, 70.8, 67.6, 53.5, 49.5, 49.5, 37.5, 24.9, 12.0, 12.0. LRMS (FAB) m/z 497 (M + H$^+$). HRMS (FAB) calcd for $C_{31}H_{37}N_4O_2$ (M + H$^+$): 497.2911; found 497.2906.

*N-(4-(2-(Diethylamino)ethoxy)phenyl)-4-methyl-6-(4-(naphthalen-2-yloxy)phenyl)pyrimidin-2-amine (**49**).* Chloropyrimidine **28** (20 mg, 0.06 mmol) afforded 16 mg (53%) of amine **53** as a yellow oil. ^{1}H NMR (300 MHz, CD_3OD) δ 8.11 (d, 2H, J = 8.8 Hz), 7.91−7.84 (m, 2H), 7.75−7.72 (m, 1H), 7.64 (d, 2H, J = 9.0 Hz), 7.46−7.40 (m, 3H), 7.25 (dd, 1H, J = 2.5, 8.9 Hz), 7.10−7.08 (m, 3H), 6.92 (d, 2H, J = 9.2 Hz), 4.12 (t, 2H, J = 5.5 Hz), 3.07 (t, 2H, J = 5.4 Hz), 2.84 (q, 4H, J = 7.2 Hz), 1.15 (t, 6H, J = 7.1 Hz). ^{13}C NMR ($CDCl_3$, 75 MHz) δ 168.3, 168.3, 164.0, 160.2, 159.6, 154.2, 134.3, 133.2, 132.3, 130.5, 130.0, 128.8, 128.8, 127.8, 127.2, 126.7, 125.0, 120.9, 120.9, 120.2, 118.6, 118.6, 115.1, 114.8, 114.8, 107.0, 66.3, 51.4, 47.5, 47.5, 24.1, 11.4, 11.4. LRMS (FAB) m/z 519 (M + H$^+$). HRMS (FAB) calcd for $C_{33}H_{35}N_4O_2$ (M + H$^+$): 519.2755; found 519.2776.

*4-(4-(Cyclohexyloxy)phenyl)-N-(4-(2-(diethylamino)ethoxy)-phenyl)-6-methylpyrimidin-2-amine (**50**).* Chloropyrimidine **21a** (20 mg, 0.07 mmol) afforded 11 mg (33%) of amine **50** as a colorless oil. ^{1}H NMR (300 MHz, CD_3OD) δ 8.03 (d, 2H, J = 9.0 Hz), 7.64 (d, 2H, J = 9.2 Hz), 7.07 (s, 1H), 6.97 (d, 2H, J = 8.8 Hz), 6.92 (d, 2H, J = 9.2 Hz), 4.41−4.36 (m, 1H), 4.11 (t, 2H, J = 5.6 Hz), 3.01 (t, 2H, J = 5.6 Hz), 2.79 (q, 4H, J = 7.2 Hz), 2.39 (s, 3H), 2.05−1.95 (m, 2H), 1.85−1.75 (m, 2H), 1.61−1.27 (m, 6H), 1.14 (t, 6H, J = 7.2 Hz). ^{13}C NMR ($CDCl_3$, 75 MHz) δ 168.0, 164.3, 160.2, 160.0, 159.5, 133.4, 129.4, 128.5, 128.5, 120.8, 120.8, 115.8, 115.8, 114.8, 114.8, 106.7, 75.4, 64.0, 51.7, 47.7, 47.7, 31.7, 31.7, 25.6, 23.7, 22.7, 22.7, 11.7, 11.7. LRMS (FAB) m/z 475 (M + H$^+$). HRMS (FAB) calcd for $C_{29}H_{39}N_4O_2$ (M + H$^+$): 475.3068; found 475.3066.

*4-(4-(Cyclohexyloxy)phenyl)-N-(3-(2-(diethylamino)ethoxy)-phenyl)-6-methylpyrimidin-2-amine (**51**).* Chloropyrimidine **21a** (20 mg, 0.07 mmol) afforded 14 mg (45%) of amine **51** as a colorless oil. ^{1}H NMR (300 MHz, CD_3OD) δ 8.07−8.02 (m, 2H), 7.73−7.72 (m, 1H), 7.19−7.17 (m, 2H), 7.09 (s, 1H), 6.08−6.94 (m, 2H), 6.58−6.52 (m, 1H), 4.39−4.33 (m, 1H), 4.12 (t, 2H, J = 5.6 Hz), 2.97 (t, 2H, J = 5.5 Hz), 2.73 (q, 4H, J = 7.2 Hz), 2.34 (s, 3H), 2.00−1.95 (m, 2H), 1.80−1.77 (m, 2H), 1.60−1.31 (m, 6H), 1.10 (t, 6H, J = 7.2 Hz). ^{13}C NMR ($CDCl_3$, 75 MHz) δ 168.1, 164.3, 160.1, 160.0, 159.5, 141.4, 129.5, 128.6, 128.6, 128.6, 115.9, 115.9, 111.3, 108,3, 107.2, 105.2, 75.4, 66.4, 51.7, 47.8, 47.8, 31.7, 31.7, 25.6, 24.3, 23.7, 23.7, 11.8, 11.8. LRMS (FAB) m/z 475 (M + H$^+$). HRMS (FAB) calcd for $C_{29}H_{39}N_4O_2$ (M + H$^+$): 475.3068; found 475.3073.

*4-(4-(2-Cyclohexylethoxy)phenyl)-N-(4-(2-(diethylamino)ethoxy)-phenyl)-6-methylpyrimidin-2-amine (**52**).* Chloropyrimidine **21b** (20 mg, 0.06 mmol) afforded 17 mg (55%) of amine **52** as a yellow oil. ^{1}H NMR (300 MHz, CD_3OD) δ 8.05 (d, 2H, J = 8.8 Hz), 7.62 (d, 2H, J = 9.2 Hz), 7.08 (s, 1H), 6.99 (d, 2H, J = 9.0 Hz), 6.91 (d, 2H, J = 9.2 Hz), 4.13−4.04 (m, 4H), 2.91 (t, 2H, J = 5.7 Hz), 2.69 (q, 4H, J = 7.1 Hz), 2.40 (s, 3H), 1.76−1.65 (m, 7H), 1.28−1.21 (m, 4H), 1.10 (t, 6H, J = 7.1 Hz). ^{13}C NMR ($CDCl_3$, 75 MHz) δ 168.0, 164.2, 161.3, 160.2, 154.2, 133.3, 129.6, 128.5, 128.5, 120.8, 120.8, 114.8, 114.8, 114.6, 114.6, 106.7, 66.6, 66.1, 51.7, 47.7, 47.7, 36.5, 34.5, 33.3, 33.3, 26.5, 26.2, 26.2, 24.3, 11.7, 11.7. LRMS (FAB) m/z 503 (M + H$^+$). HRMS (FAB) calcd for $C_{31}H_{43}N_4O_2$ (M + H$^+$): 503.3381; found 503.3371.

*4-(4-(2-Cyclohexylethoxy)phenyl)-N-(3-(2-(diethylamino)ethoxy)-phenyl)-6-methylpyrimidin-2-amine (**53**).* Chloropyrimidine **21b** (10 mg, 0.03 mmol) afforded 9 mg (58%) of amine **53** as a yellow oil. ^{1}H NMR (400 MHz, CD_3OD) δ 8.07 (d, 2H, J = 8.8 Hz), 7.74 (s, 1H), 7.20−7.17 (m, 2H), 7.11 (s, 1H), 6.98 (d, 2H, J = 8.8 Hz), 6.57−6.55 (m, 1H), 4.14 (t, 2H, J = 5.6 Hz), 4.05 (t, 2H, J = 6.5 Hz), 2.99 (t, 2H, J = 5.6 Hz), 2.74 (q, 4H, J = 7.2 Hz), 2.41 (s, 3H), 1.80−1.48 (m, 7H), 1.34−1.21 (m, 4H), 1.11 (t, 6H, J = 7.2 Hz), 1.05−0.93 (m, 2H). ^{13}C NMR ($CDCl_3$, 100 MHz) δ 168.1, 164.4, 161.4, 159.8, 159.8, 141.5, 129.7, 129.4, 128.6, 128.6, 114.7, 114.7, 107.7, 107.4, 105.2, 105.2, 66.2, 66.2, 50.6, 47.4, 47.4, 36.6, 34.6, 33.3, 33.3, 26.5, 26.2, 26.2, 24.3, 14.1, 14.1. LRMS (FAB) m/z 503 (M + H$^+$). HRMS (FAB) calcd for $C_{31}H_{43}N_4O_2$ (M + H$^+$): 503.3381; found 503.3392.

*4-(4-Chlorophenyl)-N-(3-(2-(diethylamino)ethoxy)phenyl)-6-(piperidin-1-yl)pyrimidin-2-amine (**54**).* Chloropyrimidine **16** (20 mg, 0.07 mmol) afforded 18 mg (58%) of amine **54** as a yellow oil. ^{1}H NMR (300 MHz, $CDCl_3$) δ 7.84 (d, 2H, J = 8.4 Hz), 7.49 (s, 1H), 7.34 (d, 2H, J = 8.4 Hz), 7.11 (t, 1H, J = 8.0 Hz), 6.98−6.92 (m, 2H), 6.47 (dd, 1H, J = 2.2, 8.1 Hz), 6.35 (s, 1H), 4.05 (t, 2H, J = 6.0 Hz), 3.64−3.61 (m, 4H), 2.89 (t, 2H, J = 6.0 Hz), 2.64 (q, 4H, J = 7.1 Hz), 1.62−1.58 (m, 6H), 1.04 (t, 6H, J = 7.1 Hz). ^{13}C NMR ($CDCl_3$, 75 MHz) δ 163.2, 162.9, 159.8, 159.3, 141.7, 137.3, 135.6, 129.3, 128.7, 128.7, 128.2, 128.2, 111.2, 107.9, 105.0, 91.1, 66.1, 51.6, 47.7, 47.7, 45.5, 45.5, 25.6, 25.6, 24.7, 11.7, 11.7. LRMS (FAB) m/z 480 (M + H$^+$). HRMS (FAB) calcd for $C_{27}H_{35}ClN_5O$ (M + H$^+$): 480.2525; found 480.2530.

*4-(4-Chlorophenyl)-N-(3-(2-(diethylamino)ethoxy)phenyl)-6-morpholinopyrimidin-2-amine (**55**).* Chloropyrimidine **17** (20 mg, 0.07 mmol) afforded 11 mg (34%) of amine **55** as a yellow solid. ^{1}H NMR (300 MHz, $CDCl_3$) δ 7.90 (d, 2H, J = 8.6 Hz), 7.48 (s, 1H), 7.41 (d, 2H, J = 8.4 Hz), 7.17 (t, 1H, J = 8.1 Hz), 7.05−6.99 (m, 2H), 6.55 (d, 1H, J = 8.1 Hz), 6.38 (s, 1H), 4.06 (t, 2H, J = 6.1 Hz), 3.81−3.78 (m, 4H), 3.69−3.67 (m, 4H), 2.89 (t, 2H, J = 6.0 Hz), 2.65 (q, 4H, J = 7.1 Hz), 1.07 (t, 6H, J = 7.1 Hz). LRMS (FAB) m/z 482 (M + H$^+$). ^{13}C NMR ($CDCl_3$, 125 MHz) δ 163.9, 163.5, 159.1, 159.4, 141.4, 137.0, 135.9, 129.4, 128.8, 128.8, 128.2, 128.2, 111.3, 108.1, 105.3, 90.9, 66.6, 66.6, 66.5, 51.7, 47.8, 47.8, 44.6, 44.6, 11.9. HRMS (FAB) calcd for $C_{26}H_{33}ClN_5O_2$ (M + H$^+$): 482.2317; found 482.2323.

*4-(4-Chlorophenyl)-N-(3-(2-(diethylamino)ethoxy)phenyl)-6-(4-methylpiperazin-1-yl)pyrimidin-2-amine (**56**).* Chloropyrimidine **18** (21 mg, 0.07 mmol) afforded 12 mg (37%) of amine **56** as a yellow oil. ^{1}H NMR (300 MHz, CD_3OD) δ 8.01 (d, 2H, J = 8.6 Hz), 7.61 (s, 1H), 7.42 (d, 2H, J = 8.6 Hz). 7.17−7.09 (m, 2H), 6.61 (s, 1H), 6.53−6.50 (m, 1H), 4.08 (t, 2H, J = 5.6 Hz), 3.75−3.74 (m, 4H), 2.93 (t, 2H, J = 5.5 Hz). 2.69 (q, 4H, J = 7.2 Hz), 2.53−2.50 (m, 4H), 2.32 (s, 3H), 1.10 (t, 6H, J = 7.1 Hz). ^{13}C NMR ($CDCl_3$, 75 MHz) δ 163.5, 163.3, 159.7, 159.4, 141.5, 137.1, 135.8, 129.4, 128.7, 128.7, 128.2, 128.2, 111.2, 108.0, 105.1, 91.0, 66.4, 54.7, 54.7, 51.6, 47.8, 47.8, 46.2, 44.1, 29.7, 11.8, 11.8. LRMS (FAB) m/z 495 (M + H$^+$). HRMS (FAB) calcd for $C_{27}H_{36}ClN_6O$ (M + H$^+$): 495.2634; found 495.2639.

*4-(4-Chlorophenyl)-N-(3-(2-(diethylamino)ethoxy)phenyl)-6-(1H-pyrrol-1-yl)pyrimidin-2-amine (**57**).* Chloropyrimidine **19** (25 mg, 0.09 mmol) afforded 14 mg (35%) of amine **57** as a yellow oil. ^{1}H NMR (300 MHz, CD_3OD) δ 8.14 (d, 2H, J = 8.6 Hz), 7.71−7.70 (m, 2H), 7.66 (s, 1H), 7.46 (d, 2H, J = 8.6 Hz), 7.32 (s, 1H), 7.19−7.17 (m, 2H), 6.58−6.55 (m, 1H), 6.33−6.32 (m, 2H), 4.11 (t, 2H, J = 5.6 Hz), 2.96 (t, 2H, J = 5.6 Hz), 2.72 (q, 4H, J = 7.1 Hz), 1.11 (t, 6H, J = 7.1 Hz). ^{13}C NMR ($CDCl_3$, 150 MHz) δ 165.7, 159.9, 159.5, 158.4, 140.6, 137.0, 135.7, 129.6, 129.1, 129.1, 128.4, 128.4, 118.2, 118.2, 112.5, 112.5, 111.6, 108.9, 105.7, 94.7, 66.5, 51.6, 47.8, 47.8, 11.8, 11.8. LRMS (FAB) m/z 462 (M + H$^+$). HRMS (FAB) calcd for $C_{26}H_{29}ClN_5O$ (M + H$^+$): 462.2055; found 462.2061.

*4,6-Bis(4-chlorophenyl)-N-(4-(2-(diethylamino)ethoxy)phenyl)-pyrimidin-2-amine (**58**).* Chloropyrimidine **15** (20 mg, 0.06 mmol) afforded 9 mg (30%) of amine **58** as a yellow oil. ^{1}H NMR (300 MHz, CD_3OD) δ 8.23 (d, 4H, J = 8.8 Hz), 7.74 (s, 1H), 7.71 (d, 2H, J = 9.2 Hz), 7.53 (d, 4H, J = 8.8 Hz), 6.97 (d, 2H, J = 9.0 Hz), 4.15 (t, 2H, J = 5.5 Hz), 3.07−3.05 (m, 2H), 2.82−2.79 (m, 4H), 1.16 (t, 6H, J = 7.1 Hz). ^{13}C NMR ($CDCl_3$, 125 MHz) δ 164.7, 164.7, 169.7, 154.7, 136.8, 136.8, 136.0, 136.0, 132.8, 129.1, 129.1, 129.1, 129.1, 128.4, 128.4, 128.4, 128.4, 121.3, 121.3, 114.9, 114.9, 103.6, 66.8, 51.8, 47.8, 47.8, 11.8, 11.8. LRMS (FAB) m/z 507 (M + H$^+$). HRMS (FAB) calcd for $C_{28}H_{29}Cl_2N_4O$ (M + H$^+$): 507.1713; found 507.1725.

*4,6-Bis(4-chlorophenyl)-N-(3-(2-(diethylamino)ethoxy)phenyl)-pyrimidin-2-amine (**59**).* Chloropyrimidine **15** (20 mg, 0.06 mmol) afforded 9 mg (30%) of amine **59** as a yellow oil. ^{1}H NMR (300 MHz, CD_3OD) δ 8.21 (d, 4H, J = 8.8 Hz), 7.78−7.76 (m, 1H), 7.74 (s, 1H), 7.51 (d, 4H, J = 8.8 Hz), 7.22−7.20 (m, 2H), 6.60−6.56 (m, 1H), 4.13 (t, 2H, J = 5.7 Hz), 2.96 (t, 2H, J = 5.7 Hz), 2.70 (q, 4H, J = 7.1 Hz),

1.11 (t, 6H, J = 7.1 Hz). ^{13}C NMR ($CDCl_3$, 75 MHz) δ 164.6, 164.6, 160.2, 159.5, 140.9, 136.9, 136.9, 135.7, 135.7, 129.5, 129.0, 129.0, 129.0, 129.0, 128.4, 128.4, 128.4, 128.4, 111.2, 108.7, 105.2, 103.9, 66.5, 51.7, 47.8, 47.8, 11.8, 11.8. LRMS (FAB) m/z 507 (M + H$^+$). HRMS (FAB) calcd for $C_{28}H_{29}Cl_2N_4O$ (M + H$^+$): 507.1713; found 507.1718.

*4,6-Bis(4-chlorophenyl)-N-(2-(2-(diethylamino)ethoxy)phenyl)-pyrimidin-2-amine (**60**).* Chloropyrimidine **15** (15 mg, 0.05 mmol) afforded 9 mg (39%) of amine **60** as a yellow oil. ^{1}H NMR (300 MHz, CD_3OD) δ 8.52−8.49 (m, 1H), 8.17 (d, 4H, J = 8.8 Hz), 7.74 (s, 1H), 7.50 (d, 4H, J = 8.8 Hz), 7.04−7.01 (m, 3H), 4.21 (t, 2H, J = 5.4 Hz), 3.03 (t, 2H, J = 5.4 Hz), 2.77 (q, 4H, J = 7.1 Hz), 1.16 (t, 6H, J = 7.2 Hz). ^{13}C NMR ($CDCl_3$, 100 MHz) δ 164.6, 164.6, 160.6, 146.5, 136.8, 136.8, 136.1, 136.1, 130.4, 129.0, 129.0, 129.0, 129.0, 128.5, 128.5, 128.5, 128.5, 121.7, 121.4, 119.0, 112.7, 103.7, 64.3, 51.8, 47.8, 47.8, 11.9, 11.9. LRMS (FAB) m/z 507 (M + H$^+$). HRMS (FAB) calcd for $C_{28}H_{29}Cl_2N_4O$ (M + H$^+$): 507.1713; found 507.1718.

Molecular Modeling. *Preparation of Molecular Structures.* All computational simulations were performed with the Sybyl-X 1.2 software package (Tripos, Inc., St. Louis, MO)[24] based on CentOS Linux 5.5. The structures of the compounds were prepared in the MOL2 format using the sketcher module. Gasteiger−Hückel charges were assigned to the ligand atoms. The structure of each molecule was energy optimized using the conjugate gradient method, and the optimization was terminated when the energy gradient convergence criterion reached 0.001 kcal mol^{-1} Å^{-1}. The conformer library for all compounds was stored in a database.

Preparation of the Target Protein Structure and Flexible Docking. The X-ray structure of RAGE (PDB id 3O3U) was retrieved from the PDB (Protein Data Bank). All crystallographic water molecules were removed, and the amide side chains were fixed. The active site was defined within a 3.0 Å radius of the specific amino acid residues (Lys43, Lys44, Arg48, and Arg104). The docking and subsequent scoring were performed using the default parameters of the Surflex-Dock program in Sybyl-X 1.2. The final scores for all Surflex-Dock solutions were calculated using a consensus scoring function (CScore) and then used for database ranking. After visual inspection of the docked poses, one of the conformers with a high consensus score (CScore= 5 or 4) was selected as the best docking pose that is described in the text.

Biological Study. *Preparation of Biotinylated Human RAGE and Human Aβ1−42.* Biotinylated human RAGE proteins were expressed from the pETavi plasmid in Origami2(DE3) bacteria harboring the pBirA plasmid. The recombinant RAGE proteins were extracted and purified by immobilized metal affinity chromatography, as previously described.[25] Aβ was prepared according to established protocols.[26] The Aβ stock in DMSO was diluted directly into phosphate-buffered saline (PBS) before use, and 10 μM Aβ solution in PBS was incubated for 24 h at 4 °C to generate oligomeric aggregates.

ELISA Test. One microgram of purified biotinylated human RAGE, 1 μL of 10 μM Aβ solution, and 20 μM of the compound in 100 μL of TBS-T with 2.5% BSA were incubated on a streptavidin-coated plate for 60 min at ambient temperature. After the plate was washed with TBS-T, the horseradish peroxidase conjugated 4G8 antibody (4G8-HRP, 1:1000 dilution) in 100 μL of TBS-T with 2.5% BSA was added into each well to detect the bound Aβ. The plate was incubated for 60 min at ambient temperature. After washing with TBS-T, the plate was developed with TMB substrate; the reaction was stopped with sulfuric acid. The absorbance was read on a Sunrise plate reader (TECHAN) at 450 nm.

Acute Model Study in Wild-Type Mice. ICR mice were obtained from SAMTACO (Korea). A single dose of the test compound (25 mg/kg) or vehicle was given by intraperitoneal (ip) injection to 3 month old ICR mice (25 g, n = 4, male). After 20 min, 200 μL of 25 μM human Aβ1−42 in PBS was injected into the tail vein and allowed to circulate for 30 min. Prior to sacrifice of the mice used for the determination of the amount of human Aβ in the brain, blood samples were taken from the retro-orbital plexus using EDTA-coated capillary tubes to determine the amount of circulating human Aβ.

Disease Model Study in Transgenic Mice. APPsw/PS1 mice were obtained from the Jackson Laboratory (Bar Harbor, ME). All mice were maintained on a 12-h dark and 12-h light cycle with free access to rodent chow and water. All procedures for animal tests were approved by the Medifron Animal Care and Use Committee. All surgical procedures were performed with care to minimize pain and discomfort. To evaluate the inhibitory effect of the test compounds on Aβ deposition in this AD model, the test compounds were administrated by gavage of 50 mg/(kg·day) to 6 month old male APPsw/PS1 mice (n = 4−5) until these mice reached 9 months of age. The cognitive function of each mouse was measured after 2 months of administration.

Y Maze Test. The spontaneous alternation rate was assessed using a Y-shaped plastic maze[27] (40 cm × 10 cm × 5 cm arm sizes). During 8 min sessions, the sequences of arm entries were recorded. Alternation was defined as successive entries into three arms, in overlapping triplet sets. The percent alternation was calculated as the ratio of actual alternations to possible alternations (defined as the total number of arm entries − 2) × 100%. The behavioral testing was performed in the dark phase.

ELISA of Brain Aβ. Post-mortem brains of the mice were immediately removed. The brain samples were homogenized in 3 mL of RIPA buffer (100 mM Tris, pH 8.0, 150 mM NaCl, 0.5% DOC, 1% NP-40, 0.2% SDS, and proteinase inhibitor cocktail) and sonicated for 20 s on ice. For the analyses of the soluble and insoluble Aβ1−40 and Aβ1−42 by ELISA, the brain homogenates were centrifuged for 30 min at 100 000 × g at 4 °C, after which the supernatants (RIPA-soluble fraction) were transferred into new tubes. The pellets were dissolved in 70% formic acid (FA) for 30 min and then centrifuged for 30 min at 100 000 × g at 4 °C. The supernatants (FA-soluble fraction) were transferred into new tubes. The fractions obtained by this protocol were then stored at −80 °C for determination of the Aβ levels using ELISA kits (cat. no. 27713 for 40, cat. no. 27711 for 42, IBL).

SPR Study. The experimental procedure for the SPR study followed the previously described protocol.[28] A ProteOn XPR36 system (BIO-RAD, Hercules, CA) equipped with a sensor chip was used for the real-time binding studies. TBS (25 mM Tris, 150 mM NaCl, 2 mM KCl, pH 7.4) with 0.05% Tween 20 was used as the assay running buffer and for sample preparation. Bacterially expressed biotinylated RAGE was individually immobilized onto five Neutravidin-coated channels of an NLC chip (BIO-RAD), leaving one channel blank as a reference. A 300 μL sample of biotinylated RAGE (1 μg/μL) was injected into the flow cells (30 μL/min) to allow saturation of the NLC chip by RAGE. The retention of RAGE on the sensor chip was confirmed using an anti-RAGE antibody. To perform binding kinetics analysis, 200 μL aliquots of serially diluted compounds ranging from 50 to 3.1 μM with 2% DMSO in TBS-T buffer were injected and flowed through the channels of the NLC chip for 1 min at 100 μL/min. The relationships between the response units (RU) obtained and the concentrations of the test compounds were plotted. To obtain the dissociation curves, after the analyte injection was stopped, TBS-T buffer (100 μL/min) was flowed over the chip for 400 s to dissociate the bound analytes. The ProteOn XPR36 control software ProteOn Manager v.2, provided by BIO-RAD, was used to record the changes in the RUs, to plot the binding curves, and to analyze the curves obtained from the SPR experiments.

■ ASSOCIATED CONTENT

Ⓢ Supporting Information

Validation data for ELISA assay, FSB staining of coronal section of AD model, NF-κB reporter assay on the C6 glioma cell, and purity data of the tested compounds. This material is available free charge via the Internet at http://pubs.acs.org.

AUTHOR INFORMATION

Corresponding Author

*Tel: 82-2-880-7875. Fax: 82-2-888-0649. E-mail: ygsuh@snu.ac.kr.

Notes

The authors declare no competing financial interest.

ACKNOWLEDGMENTS

This work was supported by National Research Foundation grant funded by the Korea government (MEST) as a part of Global Drug Candidate Development Program for Neurodegenerative Diseases (2011-0018334).

ABBREVIATIONS USED

RAGE, receptor for advanced glycation end products; AD, Alzheimer's disease; Aβ, amyloid-β; APP, amyloid precursor protein; BBB, blood−brain barrier; LRP-1, low-density lipoprotein receptor-related protein-1; Ig, immunoglobulin; AGE, advanced glycation end products; HMGB1, high-mobility group box-1 protein; NF-κB, nuclear factor-κB; SAR, structure−activity relationship; ELISA, enzyme-linked immunosorbent assay; SPR, surface plasmon resonance; PDB, protein data bank

REFERENCES

(1) (a) Hardy, J.; Selkoe, D. J. The amyloid hypothesis of Alzheimer's disease: Progress and problems on the road to therapeutics. *Sciences* **2002**, *297*, 353−356. (b) Aderinwale, O. G.; Ernst, H. W.; Mousa, S. A. Current therapies and new strategies for the management of Alzheimer's disease. *Am. J. Alzheimers Dis. Other Dementias* **2010**, *25*, 414−424. (c) Klafki, H.-W.; Stafenbiel, M.; Kornhuber, J.; Wiltfang, J. Therapeutic approaches to Alzheimer's disease. *Brain* **2006**, *129*, 2840−2855. (d) Rafii, M. S.; Aisen, P. S. Recent development in Alzheimer's disease. *BMC Med.* **2009**, *7*, No. 7. (e) Scarpini, E.; Scheltens, P.; Feldman, H. Treatment of Alzheimer's disease; current status and new perspectives. *Lancet Neurol.* **2003**, *2*, 539−547.

(2) (a) Tanzi, R. E.; Moir, R. D.; Wagner, S. L. Clearance of Alzheimer's Aβ peptide: The many roads to perdition. *Neuron* **2004**, *43*, 605−608. (b) Wang, Y.-J.; Zhou, H.-D.; Zhou, X.-F. Clearance of amyloid-beta in Azheimer's disease: Progress, problems and perspectives. *Drug Discovery Today* **2006**, *11*, 931−938.

(3) Neeper, M.; Schmidt, A. M.; Brett, J.; Yan, S. D.; Wang, F.; Pan, Y.-C.; Elliston, K.; Stern, D.; Shaw, A. Cloning and expression of a cell surface receptor for advanced glycosylation end products of proteins. *J. Biol. Chem.* **1992**, *267*, 14998−15004.

(4) Huttunen, H.; Fages, C.; Rauvala, H. Receptor for advanced glycation end products (RAGE)-mediated neurite outgrowth and activation of NF-κB require the cytoplasmic domain of the receptor but different downstream signaling pathways. *J. Biol. Chem.* **1999**, *274*, 19919−19924.

(5) Recent reviews about ligands of RAGE and related diseases, see: (a) Alexiou, P.; Chatzopoulou, K.; Pegklidou, K.; Demopoulos, V. J. RAGE: A multi-ligand receptor unveiling novel insights in health and disease. *Curr. Med. Chem.* **2010**, *17*, 2232−2252. (b) Barlovic, D. P.; Soro-Paavonen, A.; Jandeleit-Dahm, K. A. RAGE biology, atherosclerosis and diabetes. *Clin. Sci. (London)* **2011**, *121*, 43−55. (c) Sims, G. P.; Rowe, D. C.; Rietdijk, S. T.; Herbst, R.; Coyle, A. J. HMGB1 and RAGE in inflammation and cancer. *Annu. Rev. Immunol.* **2010**, *28*, 367−388. (d) Park, S.; Yoon, S.-J.; T, H.-J.; Shim, C. Y. RAGE and cardiovascular disease. *Front. Biosci.* **2011**, *16*, 486−497.

(6) (a) Bierhaus, A.; Schiekofer, S.; Schwaninger, M.; Andrassy, M.; Humpert, P. M.; Chen, J.; Hong, M.; Luther, T.; Henle, T.; Kloting, I.; Morcos, M.; Hofmann, M.; Tritschler, H.; Weigle, B.; Kasper, M.; Smith, M.; Perry, G.; Schmidt, A.-M.; Stern, D. M.; Haring, H.-U.; Schleicher, E.; Nawroth, P. P. Diabetes-associated sustained activation of the transcription factor nuclear factor-κB. *Diabetes* **2001**, *50*, 2792−2808. (b) Li, J.; Schmidt, A. M. Characterization and functional analysis of the promoter of RAGE, the receptor for advanced glycation end products. *J. Biol. Chem.* **1997**, *272*, 16498−16506.

(7) Deane, R.; Singh, I.; Sagare, A. P.; Bell, R. D.; Ross, N. T.; Larue, B.; Love, R.; Perry, S.; Paquette, N.; Deane, R. J.; Meenakshisundaram, T.; Zarcone, T.; Fritz, G.; Friedman, A. E.; Miller, B. L.; Zlokovic, B. V. A multimodal RAGE-specific inhibitor reduces amyloid β-mediated brain disorder in a mouse model of Alzheimer disease. *J. Clin. Invest.* **2012**, *122*, 1377−1392.

(8) Liu, G.; Garrett, M. R.; Men, P.; Zhu, X.; Perry, G.; Smith, M. G. Nanoparticle and other metal chelation thetapeutics in Alzheimer disease. *Biochim. Biophys. Acta* **2005**, *1741*, 246−252.

(9) (a) Sabbagh, M. N.; Agro, A.; Bell, J.; Aisen, P. S.; Schweizer, E.; Galasko, D. PF-04494700, an oral inhibitor of receptor for advanced glycation end products (RAGE), in Alzheimer disease. *Alzheimer Dis. Assoc. Disord.* **2011**, *25*, 206−212. (b) Srikanth, V.; Maczurek, A.; Phan, T.; Steele, M.; Westcott, B.; Juskiw, D.; Münch, G. Advanced glycation endproducts and their receptor RAGE in Alzheimer's disease. *Neurobiol. Aging* **2011**, *32*, 763−777.

(10) (a) Yammani, R. R.; Carlson, C. S.; Bresnick, A. R.; Loeser, R. F. Increase in production of matrix metalloproteinase 13 by human articular chondrocytes due to stimulation with S100A4: Role of the receptor for advanced glycation end products. *Arthritis Rheum.* **2006**, *54*, 2901−2911. (b) Yan, S. D.; Bierhaus, A.; Nawroth, P. P.; Stern, D. M. RAGE and Alzheimer's disease: A progression factor for amyloid-β-induced cellular perturbation? *J. Alzheimers Dis.* **2009**, *16*, 833−843.

(11) Matsumoto, S.; Yoshida, T.; Murata, H.; Harada, S.; Fujita, N.; Nakamura, S.; Yamamoto, Y.; Watanabe, T.; Yonekura, H.; Yamamoto, H.; Ohkubo, T.; Kobayashi, Y. Solution structure of the variable-type domain of the receptor for advanced glycation end products: New insight into AGE-RAGE interaction. *Biochemistry* **2008**, *47*, 12299−12311.

(12) (a) Münch, G.; Thome, J.; Foley, P.; Schinzel, R.; Riederer, P. Advanced glycation endproducts in ageing and Alzheimer's disease. *Brain Res. Rev.* **1997**, *23*, 134−143. (b) Reddy, V. P.; Beyaz, A. Inhibitors of the Maillard reaction and AGE breakers as therapeutics for multiple diseases. *Drug Discovery Today* **2006**, *11*, 646−654.

(13) Roschek, B., Jr.; Tallman, K. A.; Rector, C. L.; Gillmore, J. G.; Pratt, D. A.; Punta, C.; Porter, N. A. Peroxyl radical clocks. *J. Org. Chem.* **2006**, *71*, 3527−3532.

(14) Bell, I. M.; Beshore, D. C.; Gallicchio, S. N.; Williams, T. M. Efficient synthesis of 1-heterocyclic-3-aminopyrrolidinones. *Tetrahedron Lett.* **2000**, *41*, 1141−1145.

(15) (a) Delia, T. J.; Schomaker, J. M.; Kalinda, A. S. The synthesis of substituted phenylpyrimidines via Suzuki coupling reactions. *J. Heterocycl. Chem.* **2006**, *43*, 127−131. (b) Peng, Z.-H.; Journet, M.; Humphrey, G. A. Highly regioselective amination of 6-aryl-2,4-dichloropyrimidine. *Org. Lett.* **2006**, *8*, 395−398 and references therein..

(16) Mitsunobu, O.; Yamada, M.; Mukaiyama, T. Preparation of esters of phosphoric acid by the reaction of trivalent phosphorus compounds with diethyl azodicarboxylate in the presence of alcohols. *Bull. Chem. Soc. Jpn.* **1967**, *40*, 935−939.

(17) Evans, D. A.; Katz, J. L.; West, T. R. Synthesis of diary ethers through the copper-promoted arylation of phenols with aryboronic acids. An expedient synthesis of thyroxine. *Tetrahedron Lett.* **1998**, *39*, 2937−2940.

(18) Rankovic, Z.; Cai, J.; Kerr, J.; Fradera, X.; Robinson, J.; Mistry, A.; Hamilton, E.; McGarry, G.; Andrews, F.; Caulfield, W.; Cumming, I.; Dempster, M.; Waller, J.; Scullion, P.; Martin, I.; Mitchell, A.; Long, C.; Baugh, M.; Westwood, P.; Kinghorn, E.; Bruin, J.; Hamilton, W.; Uitdehaag, J.; vanZeeland, M.; Potin, D.; Saniere, L.; Fouquet, A.; Chevallier, F.; Deronzier, H.; Dorleans, C.; Nicolai, E. Design and optimization of a series of novel 2-cyano-pyrimidines as cathepsin K inhibitors. *Bioorg. Med. Chem. Lett.* **2010**, *20*, 1524−1527.

(19) Zhang, Q.; Liu, Y.; Gao, F.; Ding, Q.; Cho, C.; Hur, W.; Jin, Y.; Uno, T.; Joazerio, C. A. P.; Gray, N. Discovery of EGFR selective 4,6-disubstituted pyrimidines from a combinational kinase-directed heterocycle library. *J. Am. Chem. Soc.* **2006**, *128*, 2182−2183.

(20) Deane, R.; Yan, D. S.; Submamaryan, R. K.; LaRue, B.; Jovanovic, S.; Hogg, E.; Welch, D.; Manness, L; Lin, C.; Yu, J.; Zhu, H.; Ghiso, J.; Frangione, B.; Stern, A.; Schmidt, A. M.; Armstrong, D. L.; Arnold, B.; Liliensiek, B.; Nawroth, P.; Hofman, F.; Kindy, M.; Stern, D.; Zlokovic, B. RAGE mediates amyloid-beta peptide transport across the blood-brain barrier and accumulation in brain. *Nat. Med.* **2003**, *9*, 907−913.
(21) Reviews about soluble Aβ toxicity, see: (a) Ferreira, S. T.; Vieira, M. N.; De Felice, F. G. Soluble protein oligomers as emerging toxins in Alzheimer's and other amyloid diseases. *IUBMB Life* **2007**, *59*, 332−345. (b) Akira, K.; Hiroshi, K. Amyloid oligomers: Dynamics and toxicity in the cytosol and nucleus. *FEBS J.* **2010**, *277*, 1369−1379.
(22) Park, H.; Boyington, J. C. The 1.5 Å crystal structure of human receptor for advanced glycation endproducts (RAGE) ectodomains reveals unique features determining ligand binding. *J. Biol. Chem.* **2010**, *285*, 40762−40770.
(23) Stern, D.; Yan, S. D.; Schmidt, A. M.; Lamster, I. Ligand binding site of RAGE and uses thereof. US 2001/0053357 A1, 2001.
(24) Sybyl, 7.0 ed.; SYBYL molecular modeling software, Tripos Inc.: St. Louis, MO, 2005.
(25) Kumano-Kuramochi, M.; Xie, Q.; Sakakibara, Y.; Niimi, S.; Sekizawa, K.; Komba, S.; Machida, S. Expression and characterization of recombinant C-terminal biotinylated extracellular domain of human receptor for advanced glycation end products (hsRAGE) in *Escherichia coli*. *J. Biochem.* **2008**, *143*, 229−236.
(26) (a) Chromy, B. A.; Nowak, R. J.; Lambert, M. P.; Viola, K. L.; Chang, L.; Velasco, P. T.; Jones, B. W.; Fernandez, S. J.; Lacor, P. N.; Horowitz, P.; Finch, C. E.; Krafft, G. A.; Klein, W. L. Self-assembly of Abeta(1−42) into globular neurotoxins. *Biochemistry* **2003**, *42*, 12749−12760. (b) Dahlgren, K. N.; Manelli, A. M.; Stine, W. B., Jr.; Baker, L. K.; Krafft, G. A.; LaDu, M. J. In vitro characterization of conditions for amyloid-beta peptide oligomerization and fibrillogenesis. *J. Biol. Chem.* **2002**, *277*, 32046−32053. (c) Kayed, R.; Sokolov, Y.; Edmonds, B.; McIntire, T. M.; Milton, S. C.; Hall, J. E.; Glabe, C. G. Permeabilization of lipid bilayers is a common conformation-dependent activity of soluble amyloid oligomers in protein misfolding diseases. *J. Biol. Chem.* **2004**, *279*, 46363−46366.
(27) Melnikova, T.; Savonenko, A.; Wang, Q.; Liang, X.; Hand, T.; Wu, L.; Kaufmann, W. E.; Vehmas, A.; Andreasson, K. I. Cyclooxygenase-2 activity promotes cognitive deficits but not increased amyloid burden in a model of Alzheimer's disease in a sex-dimorphic pattern. *Neuroscience* **2006**, *141*, 1149−1162.
(28) Maezawa, I.; Hong, H. S.; Liu, R.; Wu, C. Y.; Cheng, R. H.; Kung, M. P.; Kung, H. F.; Lam, K. S.; Oddo, S.; Laferla, F. M.; Jin, L. W. Congo red and thioflavin-T analogs detect Abeta oligomers. *J. Neurochem.* **2008**, *104*, 457−468.